# GRADIENT FLOW FINITE ELEMENT DISCRETISATIONS WITH ENERGY-BASED hp-ADAPTIVITY FOR THE GROSS-PITAEVSKII EQUATION WITH ANGULAR MOMENTUM ROTATION

PASCAL HEID<sup>1,2</sup>, PAUL HOUSTON<sup>3</sup>, BENJAMIN STAMM<sup>4</sup>, AND THOMAS P. WIHLER<sup>5</sup>

ABSTRACT. This article deals with the stationary Gross-Pitaevskii non-linear eigenvalue problem in the presence of a rotating magnetic field that is used to model macroscopic quantum effects such as Bose-Einstein condensates (BECs). In this regime, the ground-state wave-function can exhibit an a priori unknown number of quantum vortices at unknown locations, which necessitates the exploitation of adaptive numerical strategies. To this end, we consider the conforming finite element method and introduce a combination of a Sobolev gradient descent that respects the energy-topology of the problem to solve the non-linearity and an hp-adaptive strategy that is solely based on energy decay rather than a posteriori error estimators for the refinement process. Numerical results demonstrate that the hp-adaptive strategy is highly efficient in terms of accuracy to compute the ground-state wave function and energy for several test problems where we observe exponential convergence.

#### 1. Introduction

In quantum physics, the Gross–Pitaevskii equation (GPE) [15, 18, 22] is widely used to study macroscopic quantum effects such as Bose–Einstein condensates (BEC), superconductivity or superfluidity. In its physical interpretation of the state of a collection of bosonic particles at zero Kelvin, or very small temperature, it can be rigorously derived from the many-body Schrödinger equation as the wave function collapses to a symmetric tensor product of a single-particle function. Such a Hartree–Fock ansatz becomes exact in the (dilute) mean-field limit, see [23,32,33] for some rigorous results.

The GPE exists both in its time-dependent and steady-state form. Within this work, we focus on the latter one with the presence of an external stirring magnetic field with magnetic vector potential  $\bf A$  that can trigger the formation of quantum vortices with a quantized vorticity. Since the number of such vortices, as well as their location, is unknown a priori, the use of adaptive finite element strategies is highly desirable. In this paper, we present a novel hp-adaptive finite element gradient flow method to minimise the Gross-Pitaevskii energy functional with the inclusion of a rotating magnetic field, given by

$$\mathsf{E}(u) := \int_{\Omega} \left( \frac{1}{2} |\nabla u|^2 + V(\mathbf{x}) |u|^2 + \frac{\beta}{2} |u|^4 - i\omega \overline{u} \left( \mathbf{A}(\mathbf{x}) \cdot \nabla u \right) \right) \, \mathrm{d}\mathbf{x}, \tag{1}$$

<sup>1)</sup> TUM School of Computation, Information, and Technlogy - Department of Mathematics, Boltz-mannstrasse 3, 85748 Garching bei München, Germany

<sup>2)</sup> University of Applied Sciences and Arts Northwestern, Bahnhofstrasse 6 5210 Windisch, Switzer-

<sup>3)</sup> School of Mathematical Sciences, University of Nottingham, University Park, Nottingham, NG7

<sup>4)</sup> Institute of Applied Analysis and Numerical Simulation, University of Stuttgart, D-70569 Stuttgart, Germany

<sup>5)</sup> Mathematics Institute, University of Bern, CH-3012 Bern, Switzerland

<sup>2010</sup> Mathematics Subject Classification. 35P30, 47J25, 49M25, 49R05, 65N25, 65N30, 65N50.

 $Key\ words\ and\ phrases.$  Variational PDE, linear and non-linear eigenvalue problems, semi-linear elliptic operators, Gross-Pitaevskii equation, momentum rotation, energy minimisation, gradient flows, iterative Galerkin procedures, adaptive finite element methods, hp-adaptivity.

on the  $L^2(\Omega)$ -unit sphere

$$S_{\mathbb{H}} := \{ v \in \mathbb{H} : ||v||_{L^{2}(\Omega)} = 1 \}.$$
 (2)

Here,  $\mathbb{H} := \mathrm{H}^1_0(\Omega; \mathbb{C})$  denotes the Sobolev space of all complex-valued  $\mathrm{H}^1$ -functions on a given bounded, connected, and open Lipschitz domain  $\Omega \subset \mathbb{R}^d$ , in dimensions  $d \in \{2,3\}$ , with vanishing trace on the boundary  $\partial\Omega$ , equipped with the inner-product

$$(u,v)_{\mathbb{H}}:=\int_{\Omega}
abla u\cdot
abla\overline{v}\,\mathrm{d}\mathbf{x}$$

and induced norm

$$||u||_{\mathbb{H}}^2 := (u, u)_{\mathbb{H}} = \int_{\Omega} |\nabla u|^2 \, d\mathbf{x}.$$
 (3)

In the energy functional (1), the (given) function  $V \in L^{\infty}(\Omega; \mathbb{R})$  represents an external potential, and  $\beta \in \mathbb{R}_{\geq 0}$  and  $\omega \in \mathbb{R}_{\geq 0}$  are prescribed non-negative constants that control the magnitude of the non-linearity and the rotation speed of the magnetic field, respectively. A thorough introduction to the basic theory and mathematical properties of ground-states of the Gross-Pitaevskii equation in a rotating frame can be found in, e.g., [9, 10, 13], which includes a discussion regarding the existence and non-existence of ground-states.

We now shortly review the most relevant literature concerning numerical methods for the approximation of solutions to the GPE equation with rotating magnetic field. The first key-question to address is whether to consider the problem as an energy minimisation problem or to solve the related non-linear eigenvalue problem that is obtained from looking at critical points of the associated Lagrangian built upon the energy functional (1) and the constraint (2). Due to the non-linear constraint, the energy minimisation can be viewed as a Riemannian energy minimisation problem. The relation between the Riemannian energy minimisation and the non-linear eigenvector problem is elaborated in [26]. The second question that arises is how to discretise the associated problem, i.e., how to represent the unknown function u in a finite-dimensional subspace of  $\mathbb{H}$ .

First, early contributions considered the imaginary time method originating from the physics literature, see, e.g., [1] where the critical angular velocities that lead to vortex formation are studied. Later, contributions of Bao et al. [11, 12, 14] introduced a mathematical framework to tackle the problem directly by energy minimisation. Different metrics to consider the Sobolev gradient of the energy functional have then been introduced in [19], while [7,20] considers conjugate gradient type methods. In [17], the authors consider a second-order flow involving the second time-derivative of the energy-functional. Very recently, Henning and Yadav contributed substantially to the analysis of the gradient descent method [29], the finite-element a priori convergence analysis [30] and the numerical study of conjugate-type gradient descents [2]. Finally, we note that the problem can also be tackled by Newton-type methods, see, e.g., [3,37] and [38] limited to the non-rotating case.

Second, the ground-state solution u can be discretised in different ways covered by standard techniques such as the finite difference [11,19] or the finite element method [1,2,12,14,19,24,29], as well as (pseudo-) spectral methods [7,11,17,20]. In the spirit of our proposed hp-strategy, which aims to design highly accurate approximation spaces with few number of degrees of freedom, are the recent approaches [27,35] based on the Localized Orthogonal Decomposition (LOD) for the case with and without rotating magnetic field, respectively.

In this paper, we propose a new hp-adaptive finite-element strategy to solve the non-linear eigenvector problem corresponding to the critical points of the energy functional (1). Our approach relies on a combination of the metric-adaptive gradient flow [28,29] and an energy-specific refinement strategy inspired from [25,31] (see also the related local error reduction approach [8] for hp-adaptive discretisations of general linear elliptic problems). The energy-based refinement strategy is considerably simpler compared to a residual-based a posteriori criteria. Further, it is important to note that within an adaptive strategy, the gradient descent can be combined with the adaptive procedure merging both iterative processes into a single unified one. With respect to [25] we present three key novel developments. First, we extend the GPE to the case with rotating magnetic field and, second, also present new analytical results on the convergence of the gradient

flow (Theorem 2.6). Third, we propose a new hp-adaptive strategy leading to much faster (exponential) convergence with respect to the number of degrees of freedom. Mesh-adaptive strategies are particularly suited in this case, since the number and location of the vortices is unknown a priori. Furthermore, high-order approximations enable the computation of very highly accurate ground-states and thus high-fidelity in the computed energies.

The outline of this paper is as follows. In Section 2, we begin by specifying the problem setting and recalling the framework of the metric-adaptive Sobolev gradient approach. Then, we prove some novel results for the gradient flow, cf. Theorem 2.6. Section 3 presents the hp-adaptive strategy, while Section 4 presents numerical experiments illustrating the performance of the proposed method. Finally, in Section 5 we summarise the work presented in this article and highlight potential future areas of research.

#### 2. Projected Sobolev gradient flow

In this section, we introduce the Gross–Pitaevskii equation for the associated minimisation problem given in (7) below, and establish the continuous and discrete projected Sobolev gradient flow for its exact and numerical solution, respectively.

2.1. Gross-Pitaevskii energy minimisation with external magnetic field. Throughout the paper, we make the following structural assumption on the external potential  $V \in L^{\infty}(\Omega; \mathbb{R})$ : (V1) We assume that

$$\delta_{\Omega} := \underset{\mathbf{x} \in \Omega}{\operatorname{ess inf}} \left( V(\mathbf{x}) - \frac{1}{2} \omega^2 |\mathbf{x}|^2 \right) > 0, \tag{4}$$

where  $\mathbf{x} = (x, y) \in \mathbb{R}^2$  and  $\mathbf{x} = (x, y, z) \in \mathbb{R}^3$ , respectively, denote the Euclidean coordinates, and  $|\cdot|$  the Euclidean norm in  $\mathbb{R}^d$ , for space dimensions d = 2, 3.

Since  $\Omega$  is a bounded domain, we note that we can always shift the potential V by a constant value so that (V1) is satisfied; indeed, this simply results in a corresponding shift of the energy. Finally, the term  $i \mathbf{A}(\mathbf{x}) \cdot \nabla$  occurring in (1), with the real-valued vector function

$$\mathbf{A}(\mathbf{x}) := \begin{cases} (y, -x)^{\top} & \text{for } \mathbf{x} = (x, y) \in \Omega \subset \mathbb{R}^2, \\ (y, -x, 0)^{\top} & \text{for } \mathbf{x} = (x, y, z) \in \Omega \subset \mathbb{R}^3, \end{cases}$$
 (5)

takes the role of the angular momentum operator; without loss of generality, for d=3, we assume that the rotation takes place about the z-axis. Since **A** is divergence-free, we note that

$$\operatorname{div}\left(\mathbf{A}|u|^{2}\right) = \mathbf{A} \cdot \nabla\left(|u|^{2}\right) = \mathbf{A} \cdot \nabla(\overline{u}u) = \overline{u}(\mathbf{A} \cdot \nabla u) + u(\mathbf{A} \cdot \nabla \overline{u});$$

hence,

$$\overline{u}(\mathbf{A} \cdot \nabla u) = \operatorname{div}(\mathbf{A}|u|^2) - u(\mathbf{A} \cdot \nabla \overline{u}).$$

From this equality, upon application of the divergence theorem and recalling that u = 0 on  $\partial\Omega$ , we infer the identity

$$\int_{\Omega} \omega \overline{u} (\mathbf{A} \cdot \nabla u) \, \mathrm{d}\mathbf{x} = - \int_{\Omega} \omega u (\mathbf{A} \cdot \nabla \overline{u}) \, \mathrm{d}\mathbf{x}.$$

Thereby, a straightforward calculation reveals that the Gross–Pitaevskii energy functional (1) can be stated equivalently as

$$\mathsf{E}(u) = \int_{\Omega} \left(\frac{1}{2} \left| -i \nabla u + \omega \mathbf{A} u \right|^2 + \left(V(\mathbf{x}) - \frac{1}{2} \omega^2 |\mathbf{x}|^2\right) |u|^2 + \frac{\beta}{2} |u|^4\right) \, \mathrm{d}\mathbf{x}.$$

In particular, this implies that the energy functional from (1) only takes real values, meaning that

$$\{\mathsf{E}(v): v \in \mathbb{H}\} \subset \mathbb{R}.\tag{6}$$

It can further be shown that there exists an element in  $\mathcal{S}_{\mathbb{H}}$ , which is not necessarily unique, at which the Gross-Pitaevskii functional E from (1) restricted to  $\mathcal{S}_{\mathbb{H}}$  attains its minimum; we provide

a proof of this result in Appendix A, thereby generalising the existence theorems of [10, 13]. In turn, the problem

$$\mathsf{E}(u_{\mathrm{GS}}) := \min_{v \in \mathcal{S}_{\mathtt{H}}} \mathsf{E}(v),\tag{7}$$

which is the focus of this paper, is well-posed (up to uniqueness). We will refer to any global minimiser of the Gross-Pitaevskii functional on the sphere  $\mathcal{S}_{\mathbb{H}}$  as a ground-state.

2.2. The Gross-Pitaevskii equation (GPE). In order to find a minimum of E under the  $L^2(\Omega)$ -normalisation constraint

$$\|u\|_{L^{2}(\Omega)}^{2} := (u, u)_{L^{2}(\Omega)} := \int_{\Omega} u\overline{u} \,d\mathbf{x} = 1,$$
 (8)

cf. (7), we consider the Lagrange functional

$$\mathsf{L}(u,\lambda) := \mathsf{E}(u) - \frac{\lambda}{2} \left( \int_{\Omega} |u|^2 \ \mathsf{d}\mathbf{x} - 1 \right).$$

Then, considering  $\mathbb{H} = \mathrm{H}^1_0(\Omega; \mathbb{C})$  as a real vector space, any (local) minimiser u of  $\mathsf{E}$  restricted to  $\mathcal{S}_{\mathbb{H}}$  satisfies the Euler–Lagrange equation

$$\langle \mathsf{E}'(u), v \rangle = \lambda \Re \left( \int_{\Omega} u \overline{v} \, \mathsf{d} \mathbf{x} \right) \quad \text{for all } v \in \mathbb{H},$$
 (9)

where  $\lambda \in \mathbb{R}$  is the Lagrange multiplier and E' denotes the *real* Gâteaux derivative of E. More precisely, E':  $\mathbb{H} \to \mathbb{H}^*$  is characterised by

$$\langle \mathsf{E}'(u), v \rangle = \left. \frac{\mathsf{d}}{\mathrm{dt}} \mathsf{E}(u + tv) \right|_{\mathbb{R} \ni t \to 0}, \qquad u, v \in \mathbb{H},$$

with  $\mathbb{H}^*$  signifying the dual space of  $\mathbb{H}$  (composed of all bounded linear forms on  $\mathbb{H}$  that map into  $\mathbb{R}$ ), and  $\langle \cdot, \cdot \rangle : \mathbb{H}^* \times \mathbb{H} \to \mathbb{R}$  the associated dual product. A simple calculation employing the Riesz representation theorem reveals that

$$\langle \mathsf{E}'(u), v \rangle = \Re \int_{\Omega} \left( \nabla u \cdot \nabla \overline{v} + 2V(\mathbf{x}) u \overline{v} + 2\beta |u|^2 u \overline{v} - 2i\omega \overline{v} (\mathbf{A}(\mathbf{x}) \cdot \nabla u) \right) \, d\mathbf{x}, \tag{10}$$

and thus, the Euler–Lagrange problem (9) consists in finding a pair  $(\lambda, u) \in \mathbb{R} \times \mathbb{H}$  such that

$$\Re \int_{\Omega} \left( \nabla u \cdot \nabla \overline{v} + 2V(\mathbf{x}) u \overline{v} + 2\beta |u|^2 u \overline{v} - 2i\omega \overline{v} (\mathbf{A}(\mathbf{x}) \cdot \nabla u) \right) \, d\mathbf{x} = \lambda \Re \left( \int_{\Omega} u \overline{v} \, d\mathbf{x} \right)$$
(11)

for all  $v \in \mathbb{H}$ . Equivalently, see [30, Prop. A.1], a solution  $(\lambda, u)$  of (11) satisfies

$$\int_{\Omega} \left( \nabla u \cdot \nabla \overline{v} + 2V(\mathbf{x}) u \overline{v} + 2\beta |u|^2 u \overline{v} - 2i\omega \overline{v} (\mathbf{A}(\mathbf{x}) \cdot \nabla u) \right) d\mathbf{x} = \lambda(u, v)_{L^2(\Omega)} \qquad \forall v \in \mathbb{H},$$
 (12)

meaning that it does not matter whether or not the real part is applied. This is the weak form of the stationary Gross-Pitaevskii equation (GPE) with angular momentum, which can also be written as a semi-linear eigenfunction problem, namely, in strong form  $(\lambda, u)$  satisfy

$$-\Delta u + 2V(\mathbf{x})u + 2\beta |u|^2 u - 2i\omega(\mathbf{A}(\mathbf{x}) \cdot \nabla u) = \lambda u \tag{13}$$

in  $\mathbb{H}^{\star}$ . An  $L^{2}(\Omega)$ -normalised solution  $u \in \mathbb{H}$  of (13) with minimal energy is termed a ground-state, denoted by  $u_{GS} \equiv u$ , cf. (7), whereas any  $L^{2}(\Omega)$ -normalised  $u \in \mathbb{H}$  solving (13), with an energy strictly higher than the ground-state energy, i.e.,  $\mathsf{E}(u) > \mathsf{E}(u_{GS}) = \min_{v \in \mathcal{S}_{\mathbb{H}}} \mathsf{E}(v)$ , is called an excited state.

Remark 2.1. The idea of using the real vector space  $\mathbb{H}$ , and, in turn, the real Gâteaux derivative of  $\mathsf{E} : \mathbb{H} \to \mathbb{R}$  for the formulation of the Euler–Lagrange equation (9), is standard practice in physics. Indeed, this is due to the fact that the mapping  $t \mapsto \mathsf{E}(u+tv)$ , for given  $u,v \in \mathbb{H}$ , takes real values only, even if t were complex, cf. (6). Consequently, by the open mapping theorem, the energy functional  $\mathsf{E}$  is not complex differentiable. Nonetheless, using the Wirtinger calculus, the weak formulation (12) can be derived in an alternative way as the Euler–Lagrange equation of the constraint minimisation problem (7).

- 2.3. **Projected Sobolev gradient flow.** In this section we aim to establish a projected Sobolev gradient flow formulation for the minimisation of the Gross-Pitaevskii energy functional E from (1). For this purpose, we will consider the real framework of the Gross-Pitaevskii equation (12) rather than the complex Hilbert space approach. We emphasise, however, that both avenues ultimately result in the identical gradient flow.
- 2.3.1. Weighted energy inner-product. In the spirit of [28–30], for given  $z \in \mathbb{H}$ , we first define the sesquilinear form

$$a_{z}(u,v) := \int_{\Omega} \left( \nabla u \cdot \nabla \overline{v} + 2V(\mathbf{x})u\overline{v} + 2\beta|z|^{2}u\overline{v} - 2i\omega\overline{v} \left( \mathbf{A}(\mathbf{x}) \cdot \nabla u \right) \right) d\mathbf{x}, \qquad u,v \in \mathbb{H}, \tag{14}$$

cf. [29, Eq. (7)], which will be investigated in the ensuing result.

**Proposition 2.2.** For any given  $z \in \mathbb{H}$ , the map  $a_z : \mathbb{H} \times \mathbb{H} \to \mathbb{C}$  from (14) defines a (complex) inner-product on the space  $\mathbb{H} = \mathrm{H}^1_0(\Omega; \mathbb{C})$ . Moreover, the induced norm is equivalent to the  $\mathbb{H}$ -norm defined in (3). In particular, for a constant c > 0 independent of  $z \in \mathbb{H}$ , the uniform coercivity property  $a_z(u, u) \geq c \|\nabla u\|_{L^2(\Omega)}^2$  for all  $u \in \mathbb{H}$  holds.

*Proof.* We will recall several ideas from [19, §2.1]. Throughout, let  $z \in \mathbb{H}$  be arbitrary.

(i) Bilinearity and symmetry. First, we note that the mapping  $u \mapsto a_z(u, v)$  is linear for any fixed  $v \in \mathbb{H}$ . Moreover, we have that  $a_z(u, v) = \overline{a_z(v, u)}$  for any  $u, v \in \mathbb{H}$ . Indeed, since  $\beta \in \mathbb{R}$  and  $V \in L^{\infty}(\Omega; \mathbb{R})$ , the conjugate-symmetry is directly observed for the first three terms in the integral from (14). Moreover, for the last term, we exploit the fact that u and v vanish along the boundary of  $\Omega$ , and hence application of the divergence theorem implies that

$$-i\omega\int_{\Omega}\overline{v}(\mathbf{A}\cdot\nabla u)\,\mathrm{d}\mathbf{x}=i\omega\int_{\Omega}u\,\mathrm{div}(\overline{v}\mathbf{A})\,\mathrm{d}\mathbf{x}=i\omega\int_{\Omega}u(\nabla\overline{v}\cdot\mathbf{A})\,\mathrm{d}\mathbf{x}=\overline{-i\omega\int_{\Omega}\overline{u}(\mathbf{A}\cdot\nabla v)\,\mathrm{d}\mathbf{x}},$$

since **A** is real-valued and divergence-free.

(ii) Coercivity and equivalence to the H-norm. We first note that

$$a_z(u,u) \le \int_{\Omega} \left( |\nabla u|^2 + (2V + 2\beta |z|^2) |u|^2 + 2\omega r_{\Omega} |\nabla u| |u| \right) d\mathbf{x},\tag{15}$$

with

$$r_{\Omega} := \sup_{\mathbf{x} \in \Omega} |\mathbf{A}(\mathbf{x})| = \sup_{\mathbf{x} \in \Omega} \sqrt{x^2 + y^2},$$

cf. (5), with  $\mathbf{x} = (x, y) \in \mathbb{R}^2$  or  $\mathbf{x} = (x, y, z) \in \mathbb{R}^3$ . Using the Cauchy-Schwarz inequality, the Rellich-Kondrachov embedding theorem, and the Poincaré-Friedrichs inequality, we observe that

$$\int_{\Omega} |z|^2 |u|^2 \, \mathrm{d}\mathbf{x} \le \|z\|_{\mathrm{L}^4(\Omega)}^2 \|u\|_{\mathrm{L}^4(\Omega)}^2 \le C \|\nabla u\|_{\mathrm{L}^2(\Omega)}^2 \|\nabla z\|_{\mathrm{L}^2(\Omega)}^2,$$

for a constant C>0 which only depends on  $\Omega$ . The remaining terms on the right-hand side of (15) can be estimated in an analogous way, so that the upper bound  $a_z(u,u) \leq C \|\nabla u\|_{\mathrm{L}^2(\Omega)}^2$  is obtained for all  $u \in \mathbb{H}$ , where the constant C>0 depends on  $\|V\|_{\mathrm{L}^\infty(\Omega)}$ ,  $\|\nabla z\|_{\mathrm{L}^2(\Omega)}$ ,  $\beta$ ,  $\omega$ , and  $\Omega$ . In order to derive the lower bound, for any  $\varepsilon \in (0,1)$  and  $\mathbf{x} \in \Omega$ , employing the arithmetic-geometric mean inequality gives

$$2|\omega \overline{u}(\mathbf{A}(\mathbf{x}) \cdot \nabla u)| \le \varepsilon |\nabla u|^2 + \varepsilon^{-1} \omega^2 r_{\Omega}^2 |u|^2. \tag{16}$$

Selecting

$$\varepsilon:=\frac{\omega^2r_\Omega^2}{\omega^2r_\Omega^2+2\delta_\Omega}\in(0,1),$$

with  $\delta_{\Omega} > 0$  from (4), it follows that  $2V(\mathbf{x}) - \varepsilon^{-1}\omega^2 r_{\Omega}^2 \ge 0$ , for (almost) all  $\mathbf{x} \in \Omega$ . Therefore, exploiting that  $\beta \ge 0$ , we have

$$c_1(\mathbf{x}) := (2V(\mathbf{x}) + 2\beta|z|^2) - \varepsilon^{-1}\omega^2 r_{\Omega}^2 \ge 0, \qquad \mathbf{x} \in \Omega.$$

$$(17)$$

Therefore, making use of (16) and (17) leads to

$$a_z(u, u) \ge \int_{\Omega} (1 - \varepsilon) |\nabla u|^2 + c_1(\mathbf{x}) |u|^2 \, d\mathbf{x} \ge c \, \|\nabla u\|_{L^2(\Omega)}^2, \tag{18}$$

where the constant is given by

$$c := 1 - \varepsilon = \frac{2\delta_{\Omega}}{\omega^2 r_{\Omega}^2 + 2\delta_{\Omega}} > 0; \tag{19}$$

cf. (4).

(iii) Finally, the positive definiteness of  $a_z$  follows directly from (18).

This complete the proof.

Upon taking the real part, we immediately obtain a real inner-product.

Corollary 2.3. The bilinear form

$$(u,v) \mapsto \Re(a_z(u,v)), \qquad u,v \in \mathbb{H},$$
 (20)

with  $a_z(\cdot,\cdot)$  from (14), defines an inner-product on the real Hilbert space  $\mathbb{H} = \mathrm{H}^1_0(\Omega;\mathbb{C})$ .

**Remark 2.4.** By definition of the inner-product  $a_u(\cdot,\cdot)$ , cf. (14), the Gross-Piteavskii eigenvalue problem can be stated equivalently as follows: find  $(\lambda, u) \in \mathbb{R} \times \mathbb{H}$  such that

$$\Re\left(a_u(u,v)\right) = \lambda \Re\left((u,v)_{\mathsf{L}^2(\Omega)}\right) \qquad \Longleftrightarrow \qquad a_u(u,v) = \lambda(u,v)_{\mathsf{L}^2(\Omega)}$$

for all  $v \in \mathbb{H}$ .

2.3.2. Energy-based orthogonal projection. The idea of the Sobolev gradient flow to be applied in this work is to follow a trajectory in the direction of the steepest descent with respect to the topology induced by the real inner-product from (20). More precisely, for fixed  $u \in \mathbb{H}$ , we define the gradient descent direction  $\nabla_{a_u} \mathsf{E}(u)$  of  $\mathsf{E}$  at  $u \in \mathbb{H}$  by

$$\Re\left(a_{u}(\nabla_{a_{u}}\mathsf{E}(u),v)\right) = \langle\mathsf{E}'(u),v\rangle \qquad \text{for all } v \in \mathbb{H}; \tag{21}$$

we emphasise that such an element  $\nabla_{a_u} \mathsf{E}(u) \in \mathbb{H}$  exists and is unique thanks to Corollary 2.3 and the Riesz representation theorem. In light of (10) and (14), we observe that

$$\Re\left(a_u(u,v)\right) = \langle \mathsf{E}'(u), v \rangle \quad \text{for any } u, v \in \mathbb{H},$$
 (22)

and thus

$$\Re \left(a_u(\nabla_{a_u}\mathsf{E}(u),v)\right) = \Re \left(a_u(u,v)\right).$$

This, in turn, implies the identity

$$\nabla_{a_{u}} \mathsf{E}(u) = u \quad \text{on } \mathbb{H}.$$
 (23)

We note that we could omit taking the real-part on the left-hand side of (21), if instead of employing the real Gâteaux derivative E' of E at u, the Wirtinger derivative were considered. This, however, would render the ensuing analysis unnecessarily more technical.

To incorporate the  $L^2(\Omega)$ -normalisation constraint (8) in the dynamical system to be specified below, we project the gradient  $\nabla_{a_u} \mathsf{E}(u) = u$  onto the linear tangent space associated to the sphere  $\mathcal{S}_{\mathbb{H}}$  from (2) at u given by

$$\mathbb{T}_u := \{ w \in \mathbb{H} : (w, u)_{L^2(\Omega)} = 0 \} = \{ w \in \mathbb{H} : \Re ((w, u)_{L^2(\Omega)}) = 0 \}.$$

Let  $P_u : \mathbb{H} \to \mathbb{T}_u$  be the orthogonal projection with respect to the inner-product  $a_u(\cdot, \cdot)$ , or equivalently to  $\Re(a_u(\cdot, \cdot))$ ; in particular, for any  $v \in \mathbb{H}$ , we have

$$a_u(\mathsf{P}_u(v), w) = a_u(v, w) \qquad \forall w \in \mathbb{T}_u.$$
 (24)

For any  $u \neq 0$ , we note the explicit formula

$$v \mapsto \mathsf{P}_{u}(v) := v - \frac{(v, u)_{\mathsf{L}^{2}(\Omega)}}{(\mathsf{G}(u), u)_{\mathsf{L}^{2}(\Omega)}} \mathsf{G}(u),$$
 (25)

where, for any  $u \in \mathbb{H}$ , the Riesz representer  $G(u) \in \mathbb{H}$  is uniquely defined by

$$a_u(\mathsf{G}(u), v) = (u, v)_{\mathsf{L}^2(\Omega)} \qquad \forall v \in \mathbb{H},$$
 (26)

or equivalently by

$$\Re\left(a_u(\mathsf{G}(u),v)\right) = \Re\left((u,v)_{\mathsf{L}^2(\Omega)}\right) \qquad \forall v \in \mathbb{H}. \tag{27}$$

**Remark 2.5.** For any  $u \in \mathbb{H}$ , we note that

$$u(\mathbf{x})\overline{\mathsf{G}(u(\mathbf{x}))} = |u(\mathbf{x})||\mathsf{G}(u(\mathbf{x}))|$$
 for a.e.  $\mathbf{x} \in \Omega$ . (28)

This follows from an argument analogous to [28, Lemma 5.5]. Specifically, from (27), we observe that G(u) is the unique minimiser of the real-valued functional

$$\mathsf{H}_u(w) := \frac{1}{2} \Re \left( a_u(w, w) \right) - \Re \left( (u, w)_{\mathsf{L}^2(\Omega)} \right), \qquad w \in \mathbb{H}$$

Hence, if we let  $\widetilde{w} := |\mathsf{G}(u)| \mathrm{e}^{i\varphi_u}$ , where  $\varphi_u \in [0, 2\pi)$  is the phase of u (i.e.,  $u = |u| \mathrm{e}^{i\varphi_u}$ ), then a straightforward calculation reveals that  $\mathsf{H}_u(\widetilde{w}) \leq \mathsf{H}_u(\mathsf{G}(u))$ . This implies that  $\widetilde{w} = \mathsf{G}(u)$  holds almost everywhere in  $\Omega$ , which directly yields (28).

2.3.3. Projected gradient flow. We introduce the dynamical system

$$\dot{u}(t) = -\mathsf{P}_{u(t)}(\nabla_{a_{u(t)}}\mathsf{E}(u(t))) = -\mathsf{P}_{u(t)}(u(t)) \quad \text{for } t > 0 \quad \text{and} \quad u(0) = u^0, \tag{29}$$

for some initial guess  $u^0 \in \mathcal{S}_{\mathbb{H}}$ , where we have employed the identity (23) in the second equality. Using the representation (25), the dynamical system (29) is given by

$$\dot{u}(t) = -\mathsf{P}_{u(t)}(u(t)) = -u(t) + \gamma_{u(t)}\mathsf{G}(u(t)), \quad t > 0, \qquad u(0) = u^0, \tag{30a}$$

where we define

$$\gamma_{u(t)} = \frac{\|u(t)\|_{L^2(\Omega)}^2}{(\mathsf{G}(u(t)), u(t))_{L^2(\Omega)}}.$$
(30b)

for some initial  $u(0) = u^0 \in \mathcal{S}_{\mathbb{H}}$ . We note that both the numerator as well as the denominator in (30b) are real-valued; in addition, taking into account (28), we observe that

$$\gamma_{u(t)} > 0 \qquad \text{if } u(t) \neq 0, \tag{31}$$

and there is no change of phase throughout the flow.

In the following result, we discuss some properties of the flow defined by the dynamical system (30). To this end, we assume that u(t) is well-defined for all  $t \ge 0$ .

**Theorem 2.6.** Given that the flow u(t) is defined for all  $t \geq 0$ , the following properties hold:

- (a) If  $u(0) = u_0 \in \mathcal{S}_{\mathbb{H}}$ , then  $u(t) \in \mathcal{S}_{\mathbb{H}}$  for all  $t \geq 0$ ;
- (b) The energy E(t) := E(u(t)) is monotone decreasing in  $t \ge 0$ ;
- (c) If  $u_0 \in \mathcal{S}_{\mathbb{H}}$ , then the flow u(t) converges to an eigenfunction  $u^* \in \mathcal{S}_{\mathbb{H}}$  of the Gross-Pitaevskii equation (13) associated with the eigenvalue given by

$$\lambda^* = \frac{1}{(\mathsf{G}_{u^*}(u^*), u^*)_{\mathsf{L}^2(\Omega)}}.$$
(32)

Proof of Theorem 2.6 (a). Due to the orthogonal projection onto the tangent space  $\mathbb{T}_u$ , the flow from (30) is  $L^2(\Omega)$ -norm preserving. Indeed, since

$$\dot{u}(t) = -\mathsf{P}_{u(t)}(u(t)) \in \mathbb{T}_{u(t)},\tag{33}$$

we find by a straightforward calculation that

$$\frac{\mathrm{d}}{\mathrm{d}t} \left\| u(t) \right\|_{\mathrm{L}^2(\Omega)}^2 = 2 \Re \left( (u(t), \dot{u}(t))_{\mathrm{L}^2(\Omega)} \right) = 0,$$

which yields the first claim.

Proof of Theorem 2.6 (b). Taking the (real) derivative of the function

$$g(t) := \mathsf{E}(u(t)), \qquad t \ge 0, \tag{34}$$

and invoking (22) implies that  $g'(t) = \langle \mathsf{E}'(u), \dot{u} \rangle = \Re(a_u(u, \dot{u}))$ , where we have suppressed the dependence of u = u(t) on t for better readability. Combining (24) and (30), we deduce that

$$g'(t) = \Re(a_u(\mathsf{P}_u(u), \dot{u})) = -\Re(a_u(\dot{u}, \dot{u})) = -a_u(\dot{u}, \dot{u}) \le 0, \tag{35}$$

cf. Proposition 2.2; i.e., the energy  $\mathsf{E}(u(t))$  is monotonically decreasing. This establishes (b).  $\square$ 

In the remaining part (c) of the proof, we may assume without loss of generality that the function g from (34) satisfies  $g'(t) \neq 0$  for all  $t \geq 0$ . Otherwise, if there exists  $t_{\star} \geq 0$  such that  $g'(t_{\star}) = 0$ , then  $u(t_{\star})$  is an eigenfunction of the GPE (12). Indeed, from (35) we deduce that  $\dot{u}(t_{\star}) = 0$ , which, upon recalling (30) and (31), leads to  $u(t_{\star}) = \lambda \mathsf{G}(u(t_{\star}))$  for  $\lambda := \Gamma(u(t_{\star})) > 0$ . In view of (26) we arrive at

$$a_{u(t_{\star})}(u(t_{\star}), v) = \lambda a_{u(t_{\star})}(\mathsf{G}(u(t_{\star})), v) = \lambda(u(t_{\star}), v)_{\mathsf{L}^{2}(\Omega)},$$

for any  $v \in \mathbb{H}$ . The proof of Theorem 2.6 (c) requires the following auxiliary result.

**Lemma 2.7.** Suppose that the solution u of (33) is  $C^2$  in time. Then, the function g from (34) satisfies the bound  $g''(t) \ge -2g'(t)$  for all t > 0.

*Proof.* For time-dependent  $\mathbb{H}$ -valued functions u, v, w, a straightforward calculation shows that

$$\frac{\mathrm{d}}{\mathrm{d}t}a_{u}(v,w) = a_{u}(\dot{v},w) + a_{u}(v,\dot{w}) + 4\beta \int_{\Omega} \Re\left(u\overline{\dot{u}}\right)v\overline{w}\,\mathrm{d}\mathbf{x},\tag{36}$$

and therefore

$$\frac{\mathrm{d}}{\mathrm{d}t}\Re(a_u(v,w)) = \Re(a_u(\dot{v},w)) + \Re(a_u(v,\dot{w})) + 4\beta\int_{\Omega}\Re\left(u\overline{\dot{u}}\right)\Re\left(v\overline{w}\right)\,\mathrm{d}\mathbf{x}.$$

Moreover, recalling (24) and (30a), for any  $v \in \mathbb{T}_u$ , where u is the solution of (33), the following holds

$$\Re(a_u(u,v)) = \Re(a_u(\mathsf{P}_u(u),v)) = -\Re(a_u(\dot{u},v)).$$

Taking the temporal derivative yields

$$\frac{\mathsf{d}}{\mathsf{d}t}\Re(a_u(u,v)) = -\frac{\mathsf{d}}{\mathsf{d}t}\Re(a_u(\dot{u},v)),$$

which, upon using (36), results in the identity

$$\Re(a_u(\dot{u},v)) + 4\beta \int_{\Omega} \Re\left(u\bar{\dot{u}}\right) \Re\left(u\bar{v}\right) \, \mathrm{d}\mathbf{x} = -\Re(a_u(\ddot{u},v)) - 4\beta \int_{\Omega} \Re\left(u\bar{\dot{u}}\right) \Re\left(\dot{u}\bar{v}\right) \, \mathrm{d}\mathbf{x},$$

for any  $v \in \mathbb{T}_u$  (independent) of time. Then, for any given t > 0, inserting  $v = \dot{u}(t) \in \mathbb{T}_{u(t)}$ , cf. (33), we deduce the equality

$$\Re(a_u(\dot{u},\dot{u})) + 4\beta \left\| \Re\left(u\overline{\dot{u}}\right) \right\|_{\mathrm{L}^2(\Omega)}^2 = -\Re(a_u(\ddot{u},\dot{u})) - 4\beta \int_{\Omega} \Re\left(u\overline{\dot{u}}\right) |\dot{u}|^2 \ \mathrm{d}\mathbf{x}.$$

Applying (35), and rearranging terms, we deduce that

$$\Re(a_u(\ddot{u},\dot{u})) = g'(t) - 4\beta \left\| \Re\left(u\overline{\dot{u}}\right) \right\|_{\mathrm{L}^2(\Omega)}^2 - 4\beta \int_{\Omega} \Re\left(u\overline{\dot{u}}\right) \left|\dot{u}\right|^2 \, \mathrm{d}\mathbf{x}.$$

Furthermore, again with the aid of (35) and (36), we have

$$g''(t) = -\frac{\mathsf{d}}{\mathsf{d}t}\Re(a_u(\dot{u},\dot{u})) = -2\Re(a_u(\ddot{u},\dot{u})) - 4\beta\int_{\Omega}\Re\left(u\overline{\dot{u}}\right)|\dot{u}|^2\;\mathsf{dx}.$$

By combining the above two equations it follows that

$$g''(t) = -2g'(t) + 8\beta \left\| \Re \left( u \overline{\dot{u}} \right) \right\|_{L^{2}(\Omega)}^{2} + 4\beta \int_{\Omega} \Re \left( u \overline{\dot{u}} \right) \left| \dot{u} \right|^{2} d\mathbf{x}. \tag{37}$$

In light of (30a), and invoking (31) and (28), we observe that

$$u\overline{\dot{u}} = u\left(-\overline{u} + \gamma_u \overline{\mathsf{G}(u)}\right) = -|u|^2 + \gamma_u|u||\mathsf{G}(u)|$$

is a real-valued function. Hence, we conclude that

$$2\Re (u\bar{u})^2 + \Re (u\bar{u}) |\dot{u}|^2 = |\dot{u}|^2 (2|u|^2 + u\bar{u}) = |\dot{u}|^2 |u| (|u| + \gamma_u |\mathsf{G}(u)|) \ge 0.$$

Exploiting this bound in (37) completes the proof.

We are now prepared to complete the proof of Theorem 2.6.

Proof of Theorem 2.6 (c). Based on Lemma 2.7, we can apply the argument pursued in the proof of [34, Thm. 7.1] to conclude that the limit  $u(t) \to u^*$  as  $t \to \infty$  exists. Moreover, upon taking the limit in (30a), we find that  $u^* = \lambda^* \mathsf{G}(u^*)$ , where

$$\lambda^{\star} = \frac{\|u^{\star}\|_{\mathrm{L}^{2}(\Omega)}^{2}}{(\mathsf{G}(u^{\star}), u^{\star})_{\mathrm{L}^{2}(\Omega)}} = \frac{1}{(\mathsf{G}(u^{\star}), u^{\star})_{\mathrm{L}^{2}(\Omega)}} > 0,$$

cf. (31). Therefore, by exploiting (26), we infer that

$$\Re\left(a_{u^{\star}}(u^{\star},v)\right) = \lambda^{\star}\Re\left(a_{u^{\star}}(\mathsf{G}(u^{\star}),v)\right) = \lambda^{\star}\Re\left((u^{\star},v)_{\mathsf{L}^{2}(\Omega)}\right) \qquad \forall v \in \mathbb{H}.$$

It now follows from Remark 2.4 that  $u^* \not\equiv 0$  is an eigenfunction of the GPE (12) with corresponding eigenvalue  $\lambda^*$ .

2.4. **Discrete gradient flow.** For the purpose of computing an approximation of the continuous gradient flow trajectory from (30), we employ the forward Euler time stepping method. Specifically, for a given initial value  $u^0 \in \mathcal{S}_{\mathbb{H}}$  this yields a sequence  $\{u^n\}_{n\geq 0} \subset \mathcal{S}_{\mathbb{H}}$  which, for  $n\geq 0$ , is defined by

$$u^{n+1} = \frac{\widehat{u}^{n+1}}{\|\widehat{u}^{n+1}\|_{L^2(\Omega)}},\tag{38a}$$

where

$$\widehat{u}^{n+1} = u^n - \tau_n \mathsf{P}_{u^n}(u^n) = (1 - \tau_n)u^n + \frac{\tau_n}{(\mathsf{G}(u^n), u^n)_{\mathsf{L}^2(\Omega)}} \mathsf{G}(u^n). \tag{38b}$$

Here,  $\{\tau_n\}_{n\geq 0}$  is a sequence of positive (discrete) time steps that is assumed to be uniformly bounded from above and below with bounds  $\tau_{\text{max}}$  and  $\tau_{\text{min}}$ , respectively, such that

$$0 < \tau_{\min} \le \tau_n \le \tau_{\max} < 2 \qquad \forall n \ge 0. \tag{39}$$

The scheme (38) is called discrete gradient flow iteration (GFI). We note that this iteration scheme coincides with the one from [29], and, up to an additional term in the weighted inner-product that incorporates the angular momentum, resembles the GFI proposed in [28, §4]. In particular, we may borrow the following result from [29, Thm. 3.3] in a modified form, which can also (largely) be obtained by following along the lines of [28, §4] (with some minor adaptations); we provide a rough sketch for the latter approach in Appendix B.

**Theorem 2.8.** For a sufficiently small lower bound  $\tau_{\min}$ , there exists a constant  $\tau_{\min} < \tau_{\max} < 2$  such that, for any sequence of time-steps  $\{\tau_n\}_n \subset [\tau_{\min}, \tau_{\max}]$ , the sequence  $\{u^n\}_n$  generated by the GFI (38a) satisfies the following properties:

(a) We have that  $\mathsf{E}(u^{n+1}) \leq \mathsf{E}(u^n)$  for all  $n \geq 0$ . Indeed, there exists a constant  $C_\tau > 0$  (depending on  $\tau_{\min}$  and  $\tau_{\max}$ ) such that

$$\mathsf{E}(u^{n+1}) - \mathsf{E}(u^n) \ge C_\tau \left\| u^{n+1} - u^n \right\|_{\mathsf{L}^2(\Omega)}^2 \tag{40}$$

for all  $n \geq 0$ .

(b) The limit  $\mathsf{E}^\star_\infty := \lim_{n \to \infty} \mathsf{E}(u^n)$  is well-defined. Moreover, there exists a strongly convergent subsequence  $\{u^{n_k}\}_k$  in  $\mathbb H$  with a limit  $u^\star_\infty \in \mathcal{S}_\mathbb H$ , and  $\mathsf{E}(u^\star_\infty) = \mathsf{E}^\star_\infty$ .

(c) Furthermore, for the limit  $u_{\infty}^{\star}$  from (b), upon defining  $\lambda_{\infty}^{\star}$  as in (32), we have that

$$a_{u_{\infty}^{\star}}(u_{\infty}^{\star}, v) = \lambda_{\infty}^{\star}(u_{\infty}^{\star}, v)_{L^{2}(\Omega)} \quad \forall v \in \mathbb{H},$$

i.e.  $(\lambda_{\infty}^{\star}, u_{\infty}^{\star})$  is a solution to the Gross-Pitaevskii EVP (13).

#### 3. hp-Adaptive Gradient Flow Finite Element Discretisation

3.1. hp-Finite element discretisation. For the purpose of a computational realisation of the discrete GFI (38), the Galerkin spaces  $\mathbb{X}_N$  will be constructed in terms of an hp-finite element approach. We focus on a sequence of conforming and shape-regular partitions  $\{\mathcal{T}_N\}_{N\in\mathbb{N}}$  of the domain  $\Omega$  into simplicial elements  $\mathcal{T}_N = \{\kappa\}_{\kappa\in\mathcal{T}_N}$  (i.e., triangles for d=2 and tetrahedra for d=3), although more general elements could also be considered. For  $N\geq 1$  and an element  $\kappa\in\mathcal{T}_N$ , we denote by  $h_\kappa:=\operatorname{diam}(\kappa)$  the diameter of  $\kappa$ . Furthermore, to each element  $\kappa\in\mathcal{T}_N$ , we associate a polynomial degree  $p_\kappa$ ,  $p_\kappa\geq 1$ , and collect these quantities in the polynomial degree vector  $\mathbf{p}_N=[p_\kappa:\kappa\in\mathcal{T}_N],\ N\geq 1$ . With this notation, for any subset  $\varpi\subset\mathcal{T}_N$ , we introduce the following hp-finite element space:

$$\mathbb{V}(\varpi, \mathbf{p}_N) := \left\{ v \in \mathbb{H} : v|_{\kappa} \in \mathbb{P}_{p_{\kappa}}(\kappa), \kappa \in \varpi, v|_{\Omega \setminus \varpi} = 0 \right\}, \tag{41}$$

where, for  $p \geq 1$ , we denote by  $\mathbb{P}_p(\kappa)$  the local space of polynomials of degree at most p on  $\kappa$ . Furthermore, similarly as before, we denote by

$$\mathcal{S}_{\mathbb{V}(\varpi,\mathbf{p}_N)} = \left\{ v \in \mathbb{V}(\varpi,\mathbf{p}_N) : \|v\|_{L^2(\Omega)} = 1 \right\}$$

the  $L^2(\Omega)$ -unit sphere in  $\mathbb{V}(\varpi, \mathbf{p}_N)$ . In the sequel, for simplicity of notation, we write  $\mathbb{X}_N := \mathbb{V}(\mathcal{T}_N, \mathbf{p}_N)$  and  $\mathcal{S}_N := \mathcal{S}_{\mathbb{V}(\mathcal{T}_N, \mathbf{p}_N)}$ . Furthermore, the restriction of the energy functional E from (1) to the Galerkin space  $\mathbb{X}_N$  is signified by  $\mathsf{E}_N := \mathsf{E}|_{\mathbb{X}_N}$ . Then, due to the compactness of the unit sphere  $\mathcal{S}_N$  in discrete spaces, there exists a (possibly non-unique) minimiser  $u_N \in \mathbb{X}_N$  of  $\mathsf{E}_N$ , i.e.,  $\mathsf{E}_N(u_N) = \min_{v \in \mathcal{S}_N} \mathsf{E}_N(v)$ , with

$$(u_N, 1)_{\mathcal{L}^2(\Omega)} \ge 0 \tag{42}$$

that satisfies the discrete GPE

$$\int_{\Omega} \left( \frac{1}{2} \nabla u_N \cdot \nabla v + V(\mathbf{x}) u_N v + \beta |u_N|^2 u_N v - i \omega v (\mathbf{A}(\mathbf{x}) \cdot \nabla u_N) \right) \, d\mathbf{x} = \lambda_N \int_{\Omega} u_N v \, d\mathbf{x} \qquad \forall v \in \mathbb{X}_N, \tag{43}$$

for some  $\lambda_N \in \mathbb{R}$ , cf. (12).

3.2. Fully discrete hp-version GFI. We now turn to the spatial discretisation of the forward Euler time-stepping gradient flow iteration (38) on the hp-finite element subspace  $\mathbb{X}_N \subset \mathbb{H}$ . To this end, for any  $u \in \mathbb{X}_N$ , we denote by  $\mathsf{G}_N(u) \in \mathbb{X}_N$  the unique solution of

$$a_u(\mathsf{G}_N(u), v) = (u, v)_{\mathsf{L}^2(\Omega)} \qquad \forall v \in \mathbb{X}_N, \tag{44}$$

or equivalently,

$$\Re (a_u(\mathsf{G}_N(u), v)) = \Re ((u, v)_{\mathsf{L}^2(\Omega)}) \qquad \forall v \in \mathbb{X}_N;$$

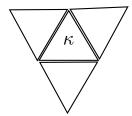
cf. (26) and (27), respectively. For given  $u \in \mathbb{X}_N$ , note that the computation of  $G_N(u)$  is a standard linear source problem: it can be solved using any appropriate linear solver at the disposal of the user. Then, for  $n \geq 0$ , the fully discrete GFI is given by

$$u_N^{n+1} = \frac{\widehat{u}_N^{n+1}}{\|\widehat{u}_N^{n+1}\|_{L^2(\Omega)}},\tag{45a}$$

where

$$\widehat{u}_N^{n+1} = (1 - \tau_N^n) u_N^n + \frac{\tau_N^n}{(\mathsf{G}_N(u_N^n), u_N^n)_{\mathsf{L}^2(\Omega)}} \mathsf{G}_N(u_N^n), \tag{45b}$$

with a sequence of discrete time steps  $\{\tau_N^n\}_{n\geq 0}$  as in (39).



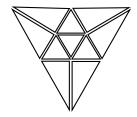


FIGURE 1. Local element patches in a triangular mesh  $\mathcal{T}_N$ ,  $N \geq 1$ , in two-dimensions. Left: Mesh patch  $\mathcal{T}_N^{\kappa}$  about an element  $\kappa$ , which consists of  $\kappa$  and its face-wise neighbours. Right: Mesh patch  $\mathcal{T}_N^{\kappa, \text{ref}}$  which is constructed based on isotropically refining  $\kappa$  (red refinement) and on a green refinement of its neighbours.

- 3.3. Competitive hp-refinements and local energy decays. In this section we pave the way for an hp-adaptivity algorithm based on employing a competitive refinement strategy on each element  $\kappa$  in the computational mesh  $\mathcal{T}_N$ ,  $N \geq 1$ . The essential idea is to compute the maximal predicted energy reduction on each element  $\kappa \in \mathcal{T}_N$ , subject to either a local h- or p-refinement. Elements with the largest maximal predicted decrease in the local energy functional are then appropriately refined. To this end, we proceed with the following steps.
- 3.3.1. Local patch refinements. For given  $N \geq 1$  and an element  $\kappa \in \mathcal{T}_N$ , we first construct the local mesh  $\mathcal{T}_N^{\kappa}$  comprising of  $\kappa$  and its immediate face-wise neighbours, cf. Fig. 1 (left). Given  $\mathcal{T}_N^{\kappa}$ , we then uniformly (red) refine element  $\kappa$  into  $n_{\kappa}$  sub-elements, where the introduction of any hanging nodes may then be removed, if desired, by introducing additional (green) refinements; we denote this locally refined mesh by  $\mathcal{T}_N^{\kappa,\text{ref}}$ , cf. Fig. 1 (right).
- 3.3.2. Local h- and p-refinements. We now outline the proposed competitive h-/p-refinements on a given finite element space  $\mathbb{X}_N = \mathbb{V}(\mathcal{T}_N, \mathbf{p}_N)$ . To this end, for an element  $\kappa \in \mathcal{T}_N$ , we construct the local mesh patches  $\mathcal{T}_N^{\kappa, \text{ref}}$  and  $\mathcal{T}_N^{\kappa}$ , as outlined above. Then, local space enrichments in terms of pure h-, respectively, p-refinement, may be considered as follows:
- (h) Given  $\kappa \in \mathcal{T}_N$ , based on the locally refined patch  $\mathcal{T}_N^{\kappa, \text{ref}}$  we construct the finite element space  $\widehat{\mathbb{V}}_{N,h}^{\kappa} := \mathbb{V}(\mathcal{T}_N^{\kappa, \text{ref}}, \mathbf{p}_h^{\kappa})$  where we define the global polynomial degree vector by

$$\left. \mathbf{p}_{\mathbf{h}}^{\kappa} \right|_{\kappa'} := \begin{cases} p_{\kappa} & \text{if } \kappa' \in \mathcal{T}_{N}^{\kappa, \mathtt{ref}}, \\ p_{\kappa'} & \text{otherwise}, \end{cases}$$

where  $p_{\kappa}$  denotes the polynomial degree on the element  $\kappa \in \mathcal{T}_N$ .

(p) Secondly, we consider the locally refined space  $\tilde{\mathbb{V}}_{N,p}^{\kappa} := \mathbb{V}(\mathcal{T}_{N}^{\kappa}, \mathbf{p}_{p}^{\kappa})$  for the element  $\kappa$  that is solely based on p-refinement, where we define a modified (global) polynomial degree vector on  $\mathcal{T}_{N}$  by

$$\mathbf{p}_{\mathbf{p}}^{\kappa}\big|_{\kappa'} := \begin{cases} p_{\kappa} + 1 & \text{if } \kappa' \in \mathcal{T}_{N}^{\kappa}, \\ p_{\kappa'} & \text{otherwise.} \end{cases}$$

We emphasise that all functions in  $\widehat{\mathbb{V}}_{N,h}^{\kappa}$  and  $\widehat{\mathbb{V}}_{N,p}^{\kappa}$  vanish outside of the local patch  $\mathcal{T}_{N}^{\kappa,\text{ref}}$ , or equivalently, on  $\mathcal{T}_{N}^{\kappa}$ , cf. (41).

3.3.3. Local energy decays. On a given mesh  $\mathcal{T}_N$ ,  $N \geq 1$ , suppose that we have obtained a sufficiently accurate approximation  $u_N^n \in \mathbb{X}_N$  of the fully discrete GPE (43), after performing  $n \geq 1$  steps of the discrete iteration (45). We now propose an hp-type refinement of the mesh  $\mathcal{T}_N$  based on a competitive local reduction strategy of the energy associated to the available approximation  $u_N^n$ . To this end, for each element  $\kappa \in \mathcal{T}_N$ , we collect the associated spaces for the proposed local h- and p-refinements, cf. above, in the set

$$\mathcal{V}_N^{\kappa} := \left\{\widehat{\mathbb{V}}_{N,\mathrm{h}}^{\kappa}\right\} \cup \left\{\widehat{\mathbb{V}}_{N,\mathrm{p}}^{\kappa}\right\}.$$

Recall that both of these spaces contain only functions that are locally supported in a vicinity of the element  $\kappa$ . Correspondingly, each space  $\widehat{\mathbb{V}}_N^{\kappa} \in \mathcal{V}_N^{\kappa}$  is spanned by some locally supported and linearly independent functions  $\xi_{\kappa}^1, \dots, \xi_{\kappa}^{m^{\kappa}}$ , namely,

$$\widehat{\mathbb{V}}_{N}^{\kappa} = \operatorname{span}\{\xi_{\kappa}^{1}, \dots, \xi_{\kappa}^{m^{\kappa}}\},\,$$

where the number of basis function  $m^{\kappa}$  depends on the underlying refinement. Then, for the proposed local h- or p-refinements, and for  $u_N^n \in \mathbb{X}_N$  as above, define the augmented space

$$\widehat{\mathbb{W}}_{N}^{\kappa}(u_{N}^{n}) := \operatorname{span}\{\xi_{\kappa}^{1}, \dots, \xi_{\kappa}^{m^{\kappa}}, u_{N}^{n}\}, \tag{46}$$

which allows us to enrich the approximate solution  $u_N^n$  by some local features on  $\kappa$  (in terms of the respective h- and p-refinements). Specifically, we perform one local fully discrete GFI-step (45) in  $\widehat{\mathbb{W}}_N^{\kappa}(u_N^n) \subset \mathbb{H}$  in order to obtain a new local approximation, denoted by  $\widetilde{u}_N^{\kappa,n} \in \widehat{\mathbb{W}}_N^{\kappa}(u_N^n)$ , with the usual constraint  $\|\widetilde{u}_N^{\kappa,n}\|_{L^2(\Omega)} = 1$ .

**Remark 3.1.** We emphasise that the augmented spaces  $\widehat{\mathbb{W}}_{N}^{\kappa}(u_{N}^{n})$ , although they feature *one global* degree of freedom due to the presence of the given approximation  $u_{N}^{n}$  as a basis function, have small dimensions. Hence, in particular, the fully discrete GFI (45) based on  $\widehat{\mathbb{W}}_{N}^{\kappa}(u_{N}^{n})$  entails hardly any computational cost and can be undertaken in parallel for each of the proposed h- and p-refinements (and for each element  $\kappa$ ).

In general, we expect the above refinements associated to an element  $\kappa \in \mathcal{T}_N$  will lead to a (local) energy decay. Here, we define

$$\Delta \mathsf{E}_{N\,\mathsf{h}}^{\kappa} := (\mathsf{E}(u_N^n) - \mathsf{E}(\widetilde{u}_N^{\kappa,n}))/\mathsf{dofs}_{\mathsf{h}}^{\kappa} \tag{47}$$

to be the potential energy reduction, per degree of freedom, when h-refinement is employed on  $\kappa$ , where  $\operatorname{dofs}_h^{\kappa}$  denotes the number of degrees of freedom present in the locally h-refined space restricted to  $\kappa$ . Similarly, the potential energy reduction, per degree of freedom, when p-refinement is utilised is given by

$$\Delta \mathsf{E}_{N,\mathrm{p}}^{\kappa} := (\mathsf{E}(u_N^n) - \mathsf{E}(\widetilde{u}_N^{\kappa,n}))/\mathrm{dofs}_{\mathrm{p}}^{\kappa},\tag{48}$$

where  $\operatorname{dofs}_p^{\kappa}$  denotes the number of degrees of freedom present in the locally p-refined space restricted to  $\kappa$ . In this way, for each element  $\kappa \in \mathcal{T}_N$ , we may compute the value

$$\Delta \mathsf{E}_{N,\max}^{\kappa} := \max \left\{ \Delta \mathsf{E}_{N,\mathrm{h}}^{\kappa}, \Delta \mathsf{E}_{N,\mathrm{p}}^{\kappa} \right\},\tag{49}$$

which indicates the maximal potential energy reduction due to the two types of refinement of the element  $\kappa$ .

Finally, we refine the set of elements  $K \in \mathcal{T}_N$  which satisfy the marking criterion

$$\Delta \mathsf{E}_{N,\max}^{\kappa} \ge \theta \max_{\kappa \in \mathcal{T}_N} \Delta \mathsf{E}_{N,\max}^{\kappa},\tag{50}$$

where  $\theta \in (0,1)$  is a fixed marking parameter. Following [21,36], cf. also [31], we set  $\theta = 1/3$ . Once the elements in the current mesh  $\mathcal{T}_N$  have been hp-refined, an hp-mesh smoother is then employed in order to construct the enriched finite element space  $\mathbb{X}_{N+1} = \mathbb{V}(\mathcal{T}_{N+1}, \mathbf{p}_{N+1})$ . This is a two-stage process: firstly, hanging nodes created through mesh refinement are removed; here, elements containing two or more hanging nodes are isotropically red refined. This process is repeated until all elements possess at most one hanging node; the remaining hanging nodes are then removed by introducing temporary (green) refinements to yield a conforming mesh  $\mathcal{T}_{N+1}$ . Subelements created through this process automatically inherit the polynomial degree of their parent. In the second step, the polynomial degree vector is smoothed by ensuring that the maximal difference in the local polynomial degree between adjacent elements is at most one; this is achieved by enriching the element with the lowest order. The above competitive hp-refinement strategy is summarised in Algorithm 1.

## **Algorithm 1** Energy-based competitive hp-adaptive refinement procedure

- 1: Input a finite element mesh  $\mathcal{T}_N$  defined on the domain  $\Omega$ , an associated polynomial degree vector  $\mathbf{p}_N$ , and a function  $u_N \in \mathbb{V}(\mathcal{T}_N, \mathbf{p}_N)$ .
- 2: for each element  $\kappa \in \mathcal{T}_N$  do
- 3: // h-refinement of  $\kappa$
- 4: Find a basis  $\{\xi_{\kappa}^1, \dots, \xi_{\kappa}^{m^{\kappa}}\}$  of the locally h-enriched space  $\widehat{\mathbb{V}}_{N,h}^{\kappa}$ .
- 5: Perform one fully discrete GFI step, cf. (45), on the local space  $\widehat{\mathbb{W}}_{N}^{\kappa}(u_{N})$  from (46), and compute the corresponding predicted energy reduction  $\Delta \mathsf{E}_{N,\mathrm{h}}^{\kappa}$ , cf. (47).
- 6: // p-refinement of  $\kappa$
- 7: Find a basis  $\{\xi_{\kappa}^{1}, \dots, \xi_{\kappa}^{\widetilde{m}^{\kappa}}\}$  of the locally *p*-enriched space  $\widehat{\mathbb{V}}_{N,p}^{\kappa}$ .
- 8: Perform one fully discrete GFI step, cf. (45), on the local space  $\widehat{\mathbb{W}}_{N}^{\kappa}(u_{N})$  from (46), and compute the corresponding predicted energy reduction  $\Delta \mathsf{E}_{N}^{\kappa}$ , cf. (48).
- 9: Compute the maximum local predicted error reduction  $\Delta \mathsf{E}_{N,\max}^{\kappa}$ , cf. (49).
- 10: end for
- 11: Determine the subset of elements K which are flagged for refinement, based on the criterion (50).
- 12: Perform h- or p-refinement on each  $\kappa \in \mathcal{K}$  according to which refinement takes the maximum in (49) and undertake hp-mesh smoothing. This results in a refined global finite element space  $\mathbb{V}(\mathcal{T}_{N+1}, \mathbf{p}_{N+1})$ .
- 3.4. hp-adaptive strategy. From a practical viewpoint, once the fully discrete GFI approximation from (45) is close to a solution of the discrete GPE (43), on a given hp-finite element space  $\mathbb{X}_N = \mathbb{V}(\mathcal{T}_N, \mathbf{p}_N)$ ,  $N \geq 1$ , we expect that any further GFI steps will no longer contribute an essential decay of the underlying energy. In this case, in order to further reduce the energy, we need to enrich the finite element space appropriately. Then, the fully discrete GFI iteration is reinitiated on the new space,  $\mathbb{X}_{N+1} = \mathbb{V}(\mathcal{T}_{N+1}, \mathbf{p}_{N+1})$ , and so on. More specifically, for  $N \geq 1$ , suppose that we have performed a reasonable number  $n \geq 1$  (possibly depending on N) of GFI-iterations (45) in  $\mathbb{X}_N$ . Consider now an hp-enriched space  $\mathbb{X}_{N+1} = \mathbb{V}(\mathcal{T}_{N+1}, \mathbf{p}_{N+1})$  as obtained by Algorithm 1. Then we may embed (or project, if refinements are not hierarchical) the final guess  $u_N^n \in \mathbb{X}_N$  on the previous space into the enriched finite element space  $\mathbb{X}_{N+1}$  in order to obtain an initial guess on

$$\mathbb{X}_N \ni u_N^n \hookrightarrow u_{N+1}^0 \in \mathbb{X}_{N+1}. \tag{51}$$

For each GFI-iteration we monitor two quantities. Firstly, we introduce the energy *increment* on each iteration given by

$$\operatorname{inc}_{N}^{n} := \mathsf{E}(u_{N}^{n-1}) - \mathsf{E}(u_{N}^{n}), \qquad n \ge 1.$$
 (52)

Secondly, we compare  $inc_N^n$  to the total energy decay on the current space  $X_N$ , i.e.,

$$dec_N^n := \mathsf{E}(u_N^0) - \mathsf{E}(u_N^n), \qquad n \ge 1. \tag{53}$$

We stop the iteration for  $n \geq 1$  as soon as  $\operatorname{inc}_N^n$  becomes small compared to  $\operatorname{dec}_N^n$ , i.e., once there is no notable (relative) benefit in performing any further discrete GFI steps on the current space  $\mathbb{X}_N$ . Specifically, for  $n \geq 1$ , this is expressed by the bound

$$\operatorname{inc}_N^n \leq \gamma \operatorname{dec}_N^n$$

for some parameter  $0 < \gamma < 1$ . We implement this procedure in Algorithm 2.

**Remark 3.2.** In practical computations, in order to guarantee a positive energy decay in each iteration step, we propose the time step strategy within (45) given by

$$\tau_N^n = \max\left\{2^{-m} : \mathsf{E}(u_N^{n+1}(2^{-m})) < \mathsf{E}(u_N^n), m \ge 0\right\}, \qquad n \ge 0.$$

where, for  $0 < s \le 1$ , we write  $u_N^{n+1}(s)$  to denote the output of the discrete GFI (45) based on the time step  $\tau_N^n = s$  and on the previous approximation  $u_N^n$ . We have observed in several examples that for the choice  $\tau_N^0 = 1$ , i.e., using m = 0 above, no time correction was needed. For that

#### **Algorithm 2** hp-Adaptive fully discrete finite element gradient flow iteration

```
1: Prescribe three parameters \theta = 1/3, \gamma \in (0,1), and 0 < \text{tol} \ll 1.
 2: Choose a sufficiently fine initial mesh \mathcal{T}_0, and an initial guess u_0^0 \in \mathcal{S}_{\mathbb{H}} with (u_0^0, 1)_{L^2(\Omega)} \geq 0,
     cf. (42). Set N := 0.
 3: loop
          Set n := 1, perform one fully discrete GFI-step (45) on \mathbb{X}_N to obtain u_N^1 \in \mathbb{X}_N.
 4:
          Compute the indicator \operatorname{inc}_N^1 (which equals \operatorname{dec}_N^1) from (52).
 5:
          while \operatorname{inc}_N^n > \gamma \operatorname{dec}_N^n \operatorname{do}
 6:
 7:
               Update n \leftarrow n + 1.
               Perform one GFI-step (45) in \mathbb{X}_N to obtain u_N^n (from u_N^{n-1}). Compute the indicators \operatorname{inc}_N^n and \operatorname{dec}_N^n from (52) and (53), respectively.
 8:
 9:
          end while
10:
          if dec_N^n > tol E(u_N^n) then
11:
               MARK and adaptively hp-REFINE the mesh \mathcal{T}_N using Algorithm 1 in order to generate
12:
               a new mesh \mathcal{T}_{N+1}.
               Define u_{N+1}^0 \in \mathbb{X}_{N+1} from u_N^n \in \mathbb{X}_N by canonical embedding (or by projection), cf. (51). Update N \leftarrow N+1.
13:
14:
15:
               return u_N^n.
16:
17:
          end if
18: end loop
```

reason, and for the sake of keeping the computational cost minimal, we fix the time step  $\tau = 1$  in the local one-step GFI in Algorithm 1; we use, however, the time step strategy for the global GFI in Algorithm 2.

#### 4. Numerical Experiments

In this section, we present a series of numerical experiments to investigate the practical performance of the proposed hp-refinement algorithm outlined in Algorithms 1 & 2. Throughout this section, we set  $\theta = 1/3$ , cf. above, and  $\gamma = 10^{-3}$ . The selection of tol is problem dependent in order to compute a highly accurate value of the ground-state energy for the example at hand. Throughout this section we compare the performance of the proposed hp-adaptive refinement strategy with the corresponding algorithm based on exploiting only local mesh subdivision, i.e., h-refinement, cf. [25]. Furthermore, to compute the solution of the underlying linear problem (44), we employ the direct MUltifrontal Massively Parallel Solver (MUMPS), see [4-6].

- 4.1. **GPE** without angular momentum operator  $\omega=0$ . Firstly, we consider a series of numerical examples where the angular momentum operator is omitted, i.e., when  $\omega=0$ . In particular, we demonstrate the performance of the proposed hp-adaptive refinement algorithm on a series of examples presented in [25]. Throughout this section, we select the initial ground-state  $u_0^0 \in \mathbb{X}_0 \subset \mathbb{H}$ , such that  $u_0^0(\mathbf{x}) = c$  for any node  $\mathbf{x}$  in the interior of the initial mesh  $\mathcal{T}_0$ , where, c>0 is the appropriate real constant which fulfils the norm constraint  $\|u_0^0\|_{L^2(\Omega)}=1$ .
- 4.1.1. Non-linear GPE with harmonic confinement potential. In this first example we consider a non-linear Bose-Einstein condensate with  $\beta=1000,\ V=^1/2(x^2+y^2),\ (\omega=0)$ , on the computational domain  $\Omega=(-6,6)^2$ . This example has been previously considered in [28] and [25], where the approximations  $\mathsf{E}(u_{\rm GS})\approx 11.9860647$  and  $\mathsf{E}(u_{\rm GS})\approx 11.98605121$  have been computed, respectively, for the energy of the ground-state. Based on employing the hp-refinement algorithm proposed in this article, cf. Algorithms 1 & 2, we compute a reference value of  $\mathsf{E}(u_{\rm GS})\approx 11.986051146671144$ . Here, the underlined digits are stable in the sense that our computations indicate that they do not change as further iterations of the hp-refinement strategy are computed.

The computed approximation to the ground-state  $u_N^n \equiv u_N \approx u_{GS}$  is depicted in Figure 2(a), the shape of which resembles an 'upside down bowl'. Furthermore, in Figure 2(b) we illustrate

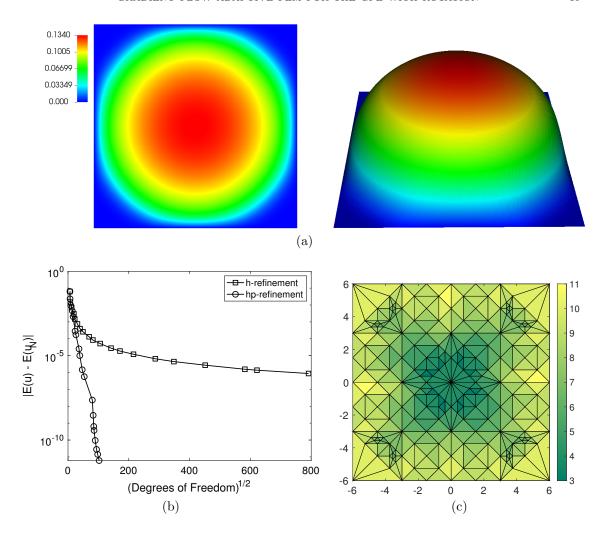


FIGURE 2. Non-linear GPE with harmonic confinement potential. (a) Computed ground-state  $u_N$ ; (b) Comparison of the error with respect to the square root of the number of degrees of freedom; (c) Final hp-mesh.

the performance of the proposed hp-adaptive algorithm, cf. Algorithms 1 & 2. Here, we plot the error of the energy  $\mathsf{E}(u_N) - \mathsf{E}(u_{\mathrm{GS}})$  against the square root of the number of degrees of freedom employed within the finite element space  $\mathbb{X}_N$ , on a linear-log scale, based on employing both h- and hp-refinement. We observe that the hp-refinement algorithm leads to an exponential decay in the error of the approximated ground-state energy as the finite element space  $\mathbb{X}_N$  is adaptively enriched: indeed, on a linear-log plot, the convergence line is roughly straight. Moreover, we observe the superiority of hp-refinement in comparison with a standard h-refinement algorithm, cf. [25], in the sense that the former refinement strategy leads to several orders of magnitude reduction in the error in  $\mathbb{E}$ , for a given number of degrees of freedom, than the corresponding quantity computed exploiting mesh subdivision only.

Finally, in Figure 2(c) we show the final hp-refined mesh generated by the proposed refinement strategy. Here we observe that some h-refinement has been undertaken around the base of the (upside down) bowl profile of the ground-state, as well as in the centre of the domain. The polynomial degree has then been enriched where the ground-state has steep gradients, as we would expect.

4.1.2. Non-linear GPE with optical lattice potential. In this second example, we consider a more challenging problem with an oscillating potential function V; to this end, we select  $\Omega = (-6,6)^2$ ,

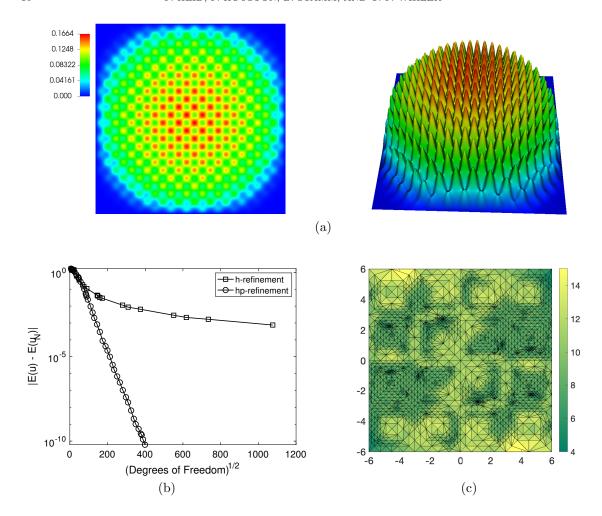


FIGURE 3. Non-linear GPE with optical lattice potential. (a) Computed ground-state  $u_N$ ; (b) Comparison of the error with respect to the square root of the number of degrees of freedom; (c) Final hp-mesh.

 $\beta = 1000$ ,  $V = 1/2(x^2+y^2)+20+20\sin(2\pi x)\sin(2\pi y)$ , and again  $\omega = 0$ . The computed approximation to the ground-state is depicted in Figure 3(a); in this setting  $u_{\rm GS}$  resembles a 'hedgehog' structure consisting of a large number of very thin spikes. Computations undertaken in [28] and [25] give values of the ground-state energy  $E(u_{\rm GS}) \approx 30.40965$  and  $E(u_{\rm GS}) \approx 30.387533$ , respectively. Based on exploiting hp-adaptivity, we have computed a reference value of  $E(u_{\rm GS}) \approx 30.387414573632611$ .

The performance of the proposed hp—refinement algorithm is depicted in Figure 3(b); here, again we observe exponential convergence of the error in the computed ground-state energy, despite the fine scale structures present in the ground-state. Moreover, hp—refinement clearly outperforms its h—version counterpart. The final hp—mesh shown in Figure 3(c) indicates that some h—refinement is necessary across most of the domain, with again p—enrichment being undertaken in smooth regions.

4.1.3. Non-linear energy functional with a nonsymmetric potential V. The final example before we consider the addition of angular momentum involves employing the nonsymmetric potential  $V=\frac{1}{2}\left(x^2+y^2+8\exp(-(x-1)^2-y^2)\right)$ , with  $\beta=200$  and  $\omega=0$  posed on the domain  $\Omega=(-8,8)^2$ , cf. [11] and [25] who computed the approximations  $\mathsf{E}(u_{\rm GS})\approx 5.8507$  and  $\mathsf{E}(u_{\rm GS})\approx 5.85058738$ , respectively. Here, we have computed  $\mathsf{E}(u_{\rm GS})\approx 5.8505871135151475$ . The ground-state consists of a single hill with a small circular region removed, cf. Figure 4(a).

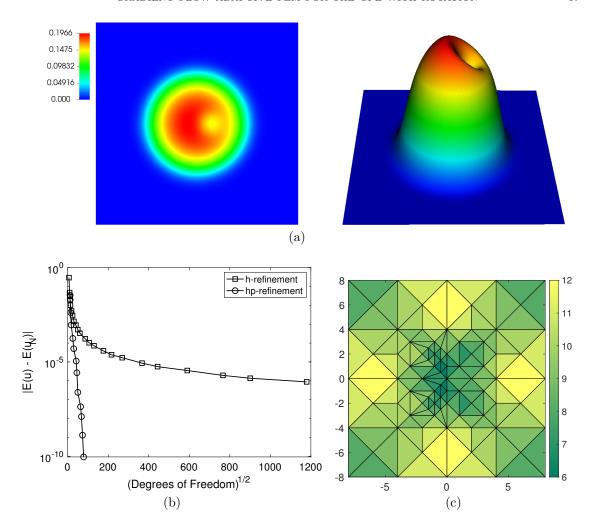


FIGURE 4. Non-linear GPE with a nonsymmetric potential V. (a) Computed ground-state  $u_N$ ; (b) Comparison of the error with respect to the square root of the number of degrees of freedom; (c) Final hp-mesh.

Figure 4(b) again highlights the potential benefits of employing hp-adaptivity: exponential convergence of the error in the computed ground-state energy is observed, as well as its superiority in terms of the computed error versus the number of degrees of freedom employed, when compared with mesh subdivision (h-refinement). The final hp-mesh depicted in Figure 4(c) highlights that some h-refinement is necessary around the top of the hill, while largely p-enrichment is undertaken elsewhere.

4.2. **GPE** with angular momentum operator  $\omega > 0$ . Finally, in this section, we now turn our attention to the case when the angular momentum operator is present in the underlying energy functional, i.e., when  $\omega > 0$ . To this end, we set  $\Omega = (-L, L)$ , for some L > 0,  $V = 1/2(x^2 + y^2)$ , and consider the range of  $\omega$  and  $\beta$ , for a given L, presented in Table 1. In addition, here we report the minimal energy computed using the proposed hp-refinement algorithm based on selecting the initial condition

$$u^{0}(x,y) = \frac{(1-\omega)\varphi_{0}(x,y) + \omega(x+iy)\varphi_{0}(x,y)}{\|(1-\omega)\varphi_{0}(x,y) + \omega(x+iy)\varphi_{0}(x,y)\|_{L^{2}(\Omega)}},$$
$$\varphi_{0}(x,y) = \frac{1}{\sqrt{\pi}} \exp\left(-(x^{2}+y^{2})/2\right),$$

where

$\omega$		β	L	$E(u_{\mathrm{GS}})$
0.5	5	10	6	1.5923190246813326
0.7	5	100	6	3.3810277420947901
0.8	3	500	10	6.0997439947822603
0.9	9	1000	12	$\overline{6.3609757543503642}$
			'	'

Table 1. Energy functional values for  $\omega > 0$ .

with zero boundary conditions, cf. [13, 20, 37]. We remark that the dependence on the computed ground-state on the choice of  $u^0$  has been studied, for example, in [13,37]; both articles recommend the selection of  $u^0$  above (or its complex conjugate), particularly for large  $\omega$ . Various values for the ground-state energy have been computed in the literature; in particular, [13] computed  $\mathsf{E}(u_{\rm GS}) \approx 1.5914$  and  $\mathsf{E}(u_{\rm GS}) \approx 3.371$  for the cases  $\omega = 0.5$ ,  $\beta = 10$  and  $\omega = 0.75$ ,  $\beta = 100$ , respectively. From [37], for  $\omega = 0.8$  and  $\beta = 500$  values of  $\mathsf{E}(u_{\rm GS})$  in the range [6.0997, 6.1055] were computed. Finally, when  $\omega = 0.9$ , and  $\beta = 1000$ , a range of values  $\mathsf{E}(u_{\rm GS}) \in [6.3615, 6.3621]$  were computed in [19], and in [37]  $\mathsf{E}(u_{\rm GS})$  was estimated to be in the range [6.3603, 6.3608]. We point out that the different ground-state energies have been computed using a variety of numerical methods, employing different initial conditions and at times different computational domains  $\Omega$ .

Numerical experiments for each of the values of  $\omega$  and  $\beta$  given in Table 1 are presented in Figures 5–8. As before, we show the computed ground-state, the comparison between the error in the approximated ground-state energy when employing both hp– and h–refinement, and the final hp–mesh. We note that as  $\omega$  is increased, the number of vortices present in the ground-state increases; for the case when  $\omega=0.9$  and  $\beta=1000$ , the ground-state features over 50 vortices arranged in a regular triangular lattice referred to as the Abrikosov lattice. In all cases we again observe that the proposed hp–refinement algorithm leads to exponential convergence of the error in the approximated ground-state energy; moreover, the efficiency of employing hp–refinement when compared to mesh subdivision alone is clearly highlighted. As the number of vortices increases with each of the test cases considered here, we observe that the accuracy attained for the computed ground-state energy decreases. Moreover, we also observe that more refinement of the computational mesh is necessary, before subsequent p–refinement is employed to yield exponential convergence of the error in the ground-state energy, as  $\omega$  is increased. In the simplest setting, i.e., when  $\omega=0.5$  and  $\beta=10$  we observe that the proposed hp–refinement algorithm simply defaults to polynomial enrichment only.

## 5. Conclusions

In this paper, we have considered the stationary non-linear Gross-Pitaevskii eigenvalue problem in the presence of a rotating magnetic field, which yields an intricate topology manifested by the presence of quantized vortices in the ground-state; the number and location of these vortices is unknown a priori. In particular, we have extended the energy-based adaptive finite element strategy presented in [25] in two key directions: firstly, we have considered the case when a rotating magnetic field is present in the underlying energy functional, and secondly, we have generalised the adaptivity framework to allow for hp-refinements of the underlying discrete finite element approximation space. Towards these goals, we have also presented a new result on the convergence of a projected gradient flow (Theorem 2.6) which respects the energy-based topology of the underlying problem at hand. The key feature of the proposed energy-adaptive hp-mesh refinement strategy is that it is based solely on potential energy-decay which can be computed locally and does not require sophisticated localisation schemes as is standard for residual-based a posteriori error estimators. The resulting method thereby intertwines the hp-mesh refinement iterative procedure with the iterative non-linear solver for the underlying problem within a unified framework in the sense that the numerical approximation to the non-linear problem is computed in tandem while the hp-mesh is adaptively refined. The performance of this proposed strategy is demonstrated on a diverse set of benchmark test problems that highlight the exponential convergence of the error

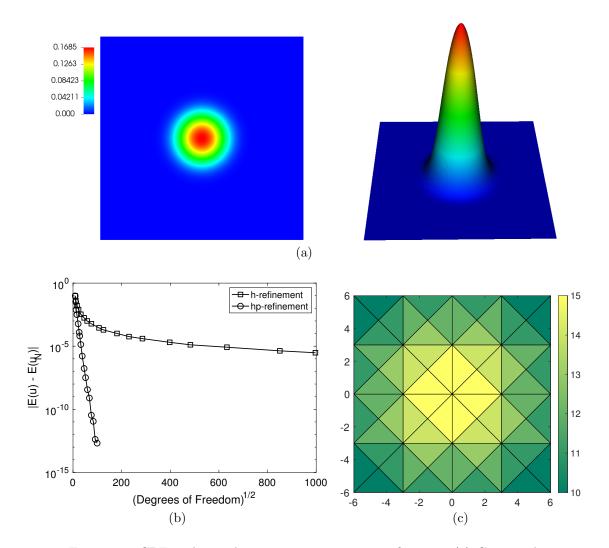


FIGURE 5. GPE with angular momentum:  $\omega = 0.5$ ,  $\beta = 10$ . (a) Computed ground-state density  $|u_N|^2$ ; (b) Comparison of the error with respect to the square root of the number of degrees of freedom; (c) Final hp-mesh.

in the computed ground-state energy with respect to the number of degrees of freedom in the resulting hp-finite element space.

#### ACKNOWLEDGMENTS

T. P. W. acknowledges the financial support of the Swiss National Science Foundation (SNF), Grant No. 200021\_212868. B. S. acknowledges funding by the Deutsche Forschungsgemeinschaft (DFG, German Research Foundation), Project No. 442047500, through the Collaborative Research Center "Sparsity and Singular Structures" (SFB 1481). Finally, we thank Eric Cancès for encouraging discussions and motivating us to extend the framework to the case with rotating magnetic field.

## APPENDIX A. EXISTENCE OF A GROUND-STATE

In the following, we verify that there exists at least one ground-state of the energy functional E from (1) under the assumption (V1). To this end, we first show that  $E : \mathbb{H} \to \mathbb{R}$  is bounded from below and coercive. Indeed, following along the lines of the proof of Proposition 2.2, we obtain

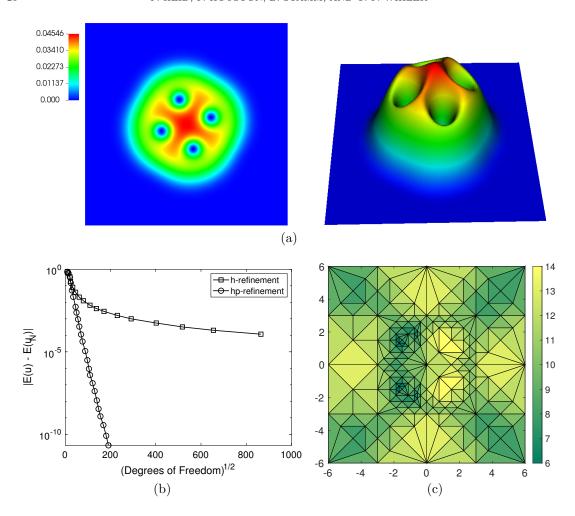


FIGURE 6. GPE with angular momentum:  $\omega = 0.75$ ,  $\beta = 100$ . (a) Computed ground-state density  $|u_N|^2$ ; (b) Comparison of the error with respect to the square root of the number of degrees of freedom; (c) Final hp-mesh.

that  $\mathsf{E}(u) \geq c/2 \|\nabla u\|_{\mathsf{L}^2(\Omega)}^2$ , with c > 0 being the constant from (19). Consequently, by the same reasoning as in the proof of [16, Lem. 2], there exists a bounded sequence  $\{u_n\}_n \subset \mathcal{S}_{\mathbb{H}}$  with

$$\lim_{n\to\infty} \mathsf{E}(u_n) = \inf_{v\in\mathcal{S}_{\mathbb{H}}} \mathsf{E}(v),$$

from which we can extract a subsequence  $\{u_{n_k}\}_k$  that converges weakly in  $\mathbb{H}$  and strongly in  $L^2(\Omega)$  to some element  $u \in \mathbb{H}$ . Due to the convergence in  $L^2(\Omega)$ , we indeed have that  $\|u\|_{L^2(\Omega)} = 1$ ; i.e.,  $u \in \mathcal{S}_{\mathbb{H}}$ . We further remark that E is weakly sequentially lower semicontinuous, since it is convex and strongly continuous; see, e.g., [39, Prop. 25.20]. Consequently, we have that

$$\mathsf{E}(u) \le \liminf_{k \to \infty} \mathsf{E}(u_{n_k}) = \inf_{v \in \mathcal{S}_{\mathbb{H}}} \mathsf{E}(v),$$

thereby implying that u is indeed a minimiser of the energy functional  $\mathsf{E}$ .

## APPENDIX B. SKETCH OF PROOF OF THEOREM 2.8

We proceed in several steps.

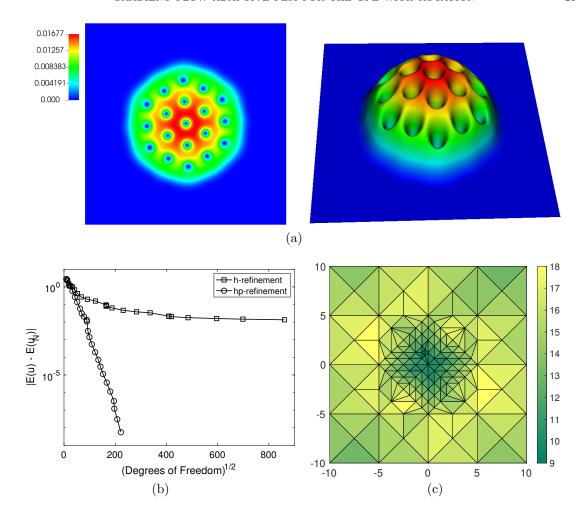


FIGURE 7. GPE with angular momentum:  $\omega = 0.8$ ,  $\beta = 500$ . (a) Computed ground-state density  $|u_N|^2$ ; (b) Comparison of the error with respect to the square root of the number of degrees of freedom; (c) Final hp-mesh.

Step 1: Firstly, a straightforward calculation reveals that the mass, without the scaling (38a), growths in each iteration step (38b). In particular, we have that

$$\|\widehat{u}^{n+1}\|_{L^{2}(\Omega)}^{2} = \|u^{n}\|_{L^{2}(\Omega)}^{2} + \|\widehat{u}^{n+1} - u^{n}\|_{L^{2}(\Omega)}^{2}.$$
 (54)

Step 2: It can further be verified that, for  $\tau_n \leq 2/5$ ,

$$\mathsf{E}(u^{n}) - \mathsf{E}(\widehat{u}^{n+1}) 
\geq -\int_{\Omega} \beta |\widehat{u}^{n+1} - u^{n}|^{4} \, \mathsf{d}\mathbf{x} + (1/\tau_{n} - 1/2) \, a_{0}(\widehat{u}^{n+1} - u^{n}, \widehat{u}^{n+1} - u^{n}).$$
(55)

Step 3: Based on (54) and (55), it can be shown by an inductive argument that there exists  $0 < \tau_{\text{max}} \le 2/5$  such that the energy decays. Indeed,

$$\mathsf{E}(u^n) - \mathsf{E}(\widehat{u}^{n+1}) \ge ca_0(\widehat{u}^{n+1} - u^n, \widehat{u}^{n+1} - u^n) \tag{56}$$

for some c > 0 independent of n, but depending on  $\tau_{\text{max}}$ . Thereby,

$$\mathsf{E}(u^{n+1}) \le \mathsf{E}(\widetilde{u}^{n+1}) \le \mathsf{E}(u^n),\tag{57}$$

where the first inequality follows from the mass growth obtained in the first step; this proves the first part of (a). Concerning (40), we simply refer to the proof in [29].

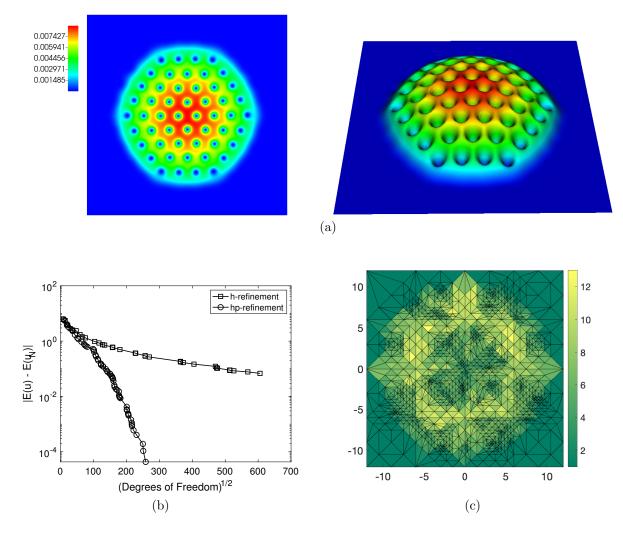


FIGURE 8. GPE with angular momentum:  $\omega = 0.9$ ,  $\beta = 1000$ . (a) Computed ground-state density  $|u_N|^2$ ; (b) Comparison of the error with respect to the square root of the number of degrees of freedom; (c) Final hp-mesh.

Step 4: By the energy decay (57) and the positivity of E, it immediately follows that  $E(u^n)$  has some limit  $E^*$ . In turn, one can show that  $u^*$  is uniformly bounded in  $\mathbb{H}$ , and thus has a weakly convergent subsequence  $\{u^{n_j}\}_j$  with limit  $u^*$ ; thanks to the Rellich-Kondrachov theorem, the convergence is strong in  $L^p(\Omega; \mathbb{C})$ , for  $1 \leq p < 6$ . Moreover, recalling (56), the convergence of the energy further implies that  $\|\hat{u}^{n+1} - u^n\|_{\mathbb{H}} \to 0$  as  $n \to \infty$ . Those convergence properties are key for all the following steps.

Step 5: Based on step 4, it can further be shown that

$$(\mathsf{G}(u^{n_j}), u^{n_j})_{\mathsf{L}^2(\Omega)} \to (\mathsf{G}(u^\star), u^\star)_{\mathsf{L}^2(\Omega)} =: (\lambda^\star)^{-1} \quad \text{as } j \to \infty,$$

and, subsequently, we have  $a_{u^*}(u^*, v) = \lambda^*(u^*, v)$  for all  $v \in \mathbb{H}$ . In particular, the claim in (c) is verified.

Step 6: A lengthy calculation discloses that  $\mathsf{E}(u^\star) = \mathsf{E}^\star$ .

Step 7: It remains to verify that the subsequence  $\{u^{n_j}\}_j$  converges to  $u^*$  strongly in  $\mathbb{H}$ . Since the proof of this claim in the present work is somewhat more involved than in the case without the angular rotation momentum, we shall provide some details. First of all, recall that  $\mathsf{E}(u^{n_j}) \to \mathsf{E}(u^*)$ ,  $u^{n_j} \to u^*$  strongly in  $L^p(\Omega)$ , for  $1 \le p < 6$ , and  $u^{n_j} \hookrightarrow u^*$  weakly

in  $\mathbb{H}$ . Consequently, we find that

$$\lim_{j\to\infty} \left(\frac{1}{2} \left\|u^{n_j}\right\|_{\mathbb{H}} - \int_{\Omega} i\omega \overline{u}^{n_j} (\mathbf{A}\cdot \nabla u^{n_j}) \,\mathrm{d}\mathbf{x}\right) = \frac{1}{2} \left\|u^\star\right\|_{\mathbb{H}} - \int_{\Omega} i\omega \overline{u^\star} (\mathbf{A}\cdot \nabla u^\star) \,\mathrm{d}\mathbf{x}.$$

In particular, if we can show that

$$\lim_{j \to \infty} \int_{\Omega} \overline{u}^{n_j} (\mathbf{A} \cdot \nabla u^{n_j}) \, d\mathbf{x} = \int_{\Omega} \overline{u^{\star}} (\mathbf{A} \cdot \nabla u^{\star}) \, d\mathbf{x}, \tag{58}$$

then  $||u^{n_j}||_{\mathbb{H}} \to ||u^*||_{\mathbb{H}}$  as  $j \to \infty$ , which in combination with the weak convergence in  $\mathbb{H}$  implies the strong convergence. Hence, it remains to verify (58). A simple manipulation reveals that

$$\begin{split} 0 & \leq \left| \int_{\Omega} \overline{u}^{n_j} (\mathbf{A} \cdot \nabla u^{n_j}) \, \mathrm{d}\mathbf{x} - \int_{\Omega} \overline{u^{\star}} (\mathbf{A} \cdot \nabla u^{\star}) \, \mathrm{d}\mathbf{x} \right| \\ & \leq \int_{\Omega} \left| u^{n_j} - u^{\star} \right| \left| \mathbf{A} \cdot \nabla u^{n_j} \right| \, \mathrm{d}\mathbf{x} + \left| \int_{\Omega} \left( \overline{u^{\star}} (\mathbf{A} \cdot \nabla u^{n_j}) \, \mathrm{d}\mathbf{x} - \overline{u^{\star}} (\mathbf{A} \cdot \nabla u^{\star}) \right) \, \mathrm{d}\mathbf{x} \right| \\ & =: I_1 + I_2. \end{split}$$

Concerning the first term, we recall that  $\{u^{n_j}\}$  is a weakly convergent sequence in  $\mathbb{H}$ , and thus is uniformly bounded. Therefore, the Cauchy–Schwarz inequality yields that

$$I_1 \le C \|u^{n_j} - u^{\star}\|_{L^2(\Omega)} \to 0 \quad \text{as } j \to \infty,$$

for some constant C>0 independent of j. To deal with the second term, we note that  $v\mapsto \int_\Omega \overline{u^\star}(\mathbf{A}\cdot\nabla v)\,\mathrm{d}\mathbf{x}$  is a linear operator on  $\mathbb{H}$ , and thus  $I_2\to 0$  as  $j\to\infty$  thanks to the weak convergence of the sequence. Together with the first part, this concludes the proof of the strong convergence.

### References

- A. Aftalion and Q. Du, Vortices in a rotating Bose-Einstein condensate: Critical angular velocities and energy diagrams in the Thomas-Fermi regime, Physical Review A 64 (2001), no. 6, 063603.
- Y. Ai, P. Henning, M. Yadav, and S. Yuan, Riemannian conjugate Sobolev gradients and their application to compute ground states of BECs, arXiv:2409.17302 (2024).
- 3. R. Altmann, P. Henning, and D. Peterseim, *The J-method for the Gross-Pitaevskii eigenvalue problem*, Numerische Mathematik **148** (2021), 575–610.
- 4. P.R. Amestoy, I.S. Duff, J. Koster, and J.-Y. L'Excellent, A fully asynchronous multifrontal solver using distributed dynamic scheduling, SIAM Journal on Matrix Analysis and Applications 23 (2001), no. 1, 15–41.
- P.R. Amestoy, I.S. Duff, and J.-Y. L'Excellent, Multifrontal parallel distributed symmetricand unsymmetric solvers, Computer Methods in Applied Mechanics and Engineering 184 (2000), 501–520.
- P.R. Amestoy, A. Guermouche, J.-Y. L'Excellent, and S. Pralet, Hybrid scheduling for the parallel solution of linear systems, Parallel Computing 32 (2006), no. 2, 136–156.
- 7. X. Antoine, A. Levitt, and Q. Tang, Efficient spectral computation of the stationary states of rotating Bose-Einstein condensates by preconditioned nonlinear conjugate gradient methods, Journal of Computational Physics 343 (2017), 92–109.
- 8. P. Bammer, A. Schröder, and T. P. Wihler, An hp-adaptive strategy based on locally predicted error reductions, arXiv report 2311.13255 (2023).
- 9. W. Bao, Mathematical models and numerical methods for Bose-Einstein condensation, Proceedings of the International Congress of Mathematicians—Seoul 2014. Vol. IV, Kyung Moon Sa, Seoul, 2014, pp. 971–996.
- W. Bao and Y. Cai, Mathematical theory and numerical methods for Bose-Einstein condensation, Kinetic & Related Models 6 (2013), no. 1.
- 11. W. Bao and Q. Du, Computing the ground state solution of Bose–Einstein condensates by a normalized gradient flow, SIAM Journal on Scientific Computing 25 (2004), no. 5, 1674–1697.
- 12. W. Bao, D. Jaksch, and P. Markowich, Numerical solution of the Gross-Pitaevskii equation for Bose-Einstein condensation, Journal of Computational Physics 187 (2003), no. 1, 318–342.
- 13. W. Bao, P. A. Markowich, and H. Wang, Ground, symmetric and central vortex states in rotating Bose–Einstein condensates, Communications in Mathematical Sciences 3 (2005), no. 1, 57–88.
- W. Bao and W. Tang, Ground-state solution of Bose-Einstein condensate by directly minimizing the energy functional, Journal of Computational Physics 187 (2003), no. 1, 230-254.
- 15. S.N. Bose, Plancks Gesetz und Lichtquantenhypothese, Zeitschrift für Physik 26 (1924), no. 1, 178–181.
- E. Cancès, R. Chakir, and Y. Maday, Numerical analysis of nonlinear eigenvalue problems, Journal of Scientific Computing 45 (2010), 90–117.

- 17. H. Chen, G. Dong, W. Liu, and Z. Xie, Second-order flows for computing the ground states of rotating Bose–Einstein condensates, Journal of Computational Physics 475 (2023), 111872.
- 18. F. Dalfovo, S. Giorgini, L.P. Pitaevskii, and S. Stringari, *Theory of Bose-Einstein condensation in trapped gases*, Reviews of Modern Physics **71** (1999), no. 3, 463.
- 19. I. Danaila and P. Kazemi, A new Sobolev gradient method for direct minimization of the Gross-Pitaevskii energy with rotation, SIAM Journal on Scientific Computing 32 (2010), no. 5, 2447–2467.
- 20. I. Danaila and B. Protas, Computation of ground states of the Gross-Pitaevskii functional via Riemannian optimization, SIAM Journal on Scientific Computing 39 (2017), no. 6, B1102-B1129.
- 21. L. Demkowicz, Computing with hp-adaptive finite elements. Vol. 1, Chapman & Hall/CRC Applied Mathematics and Nonlinear Science Series, Chapman & Hall/CRC, Boca Raton, FL, 2007, One and two dimensional elliptic and Maxwell problems, With 1 CD-ROM (UNIX). MR 2267112
- 22. A. Einstein, Quantentheorie des einatomigen idealen Gases, Sitzungsberichte der Preussischen Akademie der Wissenschafte Sitzung der physikalisch-mathematischen Klasse vom 8. Januar (1924), 261–267.
- 23. L. Erdös, B. Schlein, and H.-T. Yau, Derivation of the Gross-Pitaevskii equation for the dynamics of Bose–Einstein condensate, Annals of Mathematics (2010), 291–370.
- 24. M. Hauck, Y. Liang, and D. Peterseim, Positivity preserving finite element method for the Gross-Pitaevskii ground state: discrete uniqueness and global convergence, arXiv:2405.17090 (2024).
- 25. P. Heid, B. Stamm, and T. P. Wihler, Gradient flow finite element discretizations with energy-based adaptivity for the Gross-Pitaevskii equation, Journal of Computational Physics 436 (2021), 110165.
- 26. P. Henning and E. Jarlebring, The Gross-Pitaevskii equation and eigenvector nonlinearities: Numerical methods and algorithms, Preprint, to appear in SIAM Review (2024).
- P. Henning and A. Persson, On Optimal Convergence Rates for Discrete Minimizers of the Gross-Pitaevskii Energy in Localized Orthogonal Decomposition Spaces, Multiscale Modeling & Simulation 21 (2023), no. 3, 993-1011.
- 28. P. Henning and D. Peterseim, Sobolev gradient flow for the Gross-Pitaevskii eigenvalue problem: Global convergence and computational efficiency, SIAM Journal on Numerical Analysis 58 (2020), no. 3, 1744–1772.
- 29. P. Henning and M. Yadav, Convergence of a Riemannian gradient method for the Gross-Pitaevskii energy functional in a rotating frame, arXiv:2406.03885 (2024).
- 30. \_\_\_\_\_\_, On discrete ground states of rotating Bose-Einstein condensates, Mathematics of Computation 94 (2025), no. 351, 1–32.
- 31. P. Houston and T. P. Wihler, Adaptive energy minimisation for hp-finite element methods, Computers & Mathematics with Applications **71** (2016), no. 4, 977 990.
- 32. M. Lewin, Mean-field limit of Bose systems: rigorous results, arXiv:1510.04407 (2015).
- 33. E.H. Lieb, R. Seiringer, and J. Yngvason, Bosons in a trap: A rigorous derivation of the Gross-Pitaevskii energy functional, The Stability of Matter: From Atoms to Stars, Springer, 2001, pp. 685–697.
- 34. J. W. Neuberger, Sobolev gradients and differential equations, second ed., Lecture Notes in Mathematics, vol. 1670, Springer-Verlag, Berlin, 2010.
- 35. D. Peterseim, J. Wärnegård, and Ch. Zimmer, Super-localised wave function approximation of Bose-Einstein condensates, Journal of Computational Physics 510 (2024), 113097.
- 36. P. Solin, K. Segeth, and I. Dolezel, *Higher-order finite element methods*, Studies in advanced mathematics, Chapman & Hall/CRC, Boca Raton, London, 2004.
- 37. X. Wu, Z. Wen, and W. Bao, A regularized Newton method for computing ground states of Bose–Einstein condensates, Journal of Scientific Computing 73 (2017), no. 1, 303–329.
- 38. F. Xu, H. Xie, M. Xie, and M. Yue, A multigrid method for the ground state solution of Bose-Einstein condensates based on Newton iteration, BIT Numerical Mathematics 61 (2021), 645-663.
- 39. E. Zeidler, Nonlinear functional analysis and its applications. II/B, Springer-Verlag, New York, 1990.